

Towards Automated Discovery of Asymmetric Mempool DoS in Blockchains

Yibo Wang*, Yuzhe Tang* IEEE Member, Kai Li†, Wanning Ding*, Zhihua Yang* *Syracuse University, {ywang349,ytang100,wding04,zyang47}@syr.edu †San Diego State University, kli5@sdsu.edu

Abstract— In blockchains, mempool controls transaction flow before consensus, denial of whose service hurts the health and security of blockchain networks. This paper presents MPFUZZ, the first mempool fuzzer to find asymmetric DoS bugs by exploring the space of symbolized mempool states and optimistically estimating the promisingness of an intermediate state in reaching bug oracles. Compared to the baseline blockchain fuzzers, MPFUZZ achieves a $> 100\times$ speedup in finding known DETER exploits. Running MPFUZZ on major Ethereum clients leads to discovering new mempool vulnerabilities, which exhibit a wide variety of sophisticated patterns, including stealthy mempool eviction and mempool locking. Rule-based mitigation schemes are proposed against all newly discovered vulnerabilities.

1. INTRODUCTION

In Ethereum, a mempool buffers unconfirmed transactions from web3 users before they are included in the next blocks. Mempool provides the essential functionality to bridge the gap between varying rates of submitted transactions and rates of produced blocks, regardless of public or private transactions it serves. As shown in recent studies [1], denying a mempool service can force the blockchain to produce blocks of low or even zero (Gas) utilization, undermining validators’ incentives and shrinking the blockchain networks in the long run, re-introducing the 51% attacks. Besides, a denied mempool service can prevent normal transactions from block inclusion, cutting millions of web3 users off the blockchain and failing the decentralized applications relying on real-time blockchain access.

Problem: Spamming the mempool to deny its service has been studied for long [2]–[5]. Early designs by sending spam transactions at high prices burden attackers with high costs and are of limited practicality. What poses a real threat is Asymmetric Denial of Mempool Service, coined by ADAMS, in which the mempool service is denied at an asymmetrically low cost. That is, the attack costs, in terms of the fees of adversarial transactions, are significantly lower than those of normal transactions victimized by the denied mempool. In the existing literature, DETER [1] is the first ADAMS attack, and it works by sending invalid transactions to *directly evict* normal transactions in the mempool. MemPurge [6] is a similar mempool attack that finds a way to send overdraft transactions into Geth’s pending transaction pool and causes eviction there. These known attacks are easy to detect (i.e., following the same direct-eviction pattern). In fact, the DETER bugs reported in 2021 have been successfully fixed in all

major Ethereum clients as of Fall 2023, including Geth, Nethermind, Erigon, and Besu. Given this state of affairs, we pose the following research question: Are there new ADAMS vulnerabilities in the latest Ethereum clients already patched against direct-eviction based attacks?

This work takes a systematic and semi-automated approach to discovering ADAMS vulnerabilities, unlike the existing DETER bugs that are manually found. Fuzzing mempool implementations is a promising approach but also poses unique challenges: Unlike the consensus implementation that reads only valid confirmed transactions, the mempool, which resides in the pre-consensus phase, needs to handle various unconfirmed transactions, imposing a much larger input space for the fuzzer. For instance, a mempool can receive *invalid transactions under legitimate causes*,¹ and factors such as fees or prices are key in determining transaction admission outcomes. Existing blockchain fuzzers including Fluffy [7], Loki [8] and Tyr [9] all focus on fuzzing consensus implementation and don’t explore the extra transaction space required by mempool fuzzing. As a result, directly re-purposing a consensus fuzzer to fuzz mempool would be unable to detect the DETER bugs, let alone discover more sophisticated new ADAMS bugs.

Proposed methods: To efficiently fuzz mempools, our key observation is that real-world mempool implementation admits transactions based on abstract “symbols”, such as pending and future transactions, instead of concrete value. Thus, *sending multiple transactions under one symbol would trigger the same mempool behavior repeatedly*, and it suffices to explore just one transaction per symbol during fuzzing without losing the diversity of mempool behavior.

We propose symbolized-stateful mempool fuzzing or MPFUZZ. To begin with, MPFUZZ is set up and run in a three-step workflow: It is first manually set up against a size-reduced mempool under test, which induces a much smaller search space for fuzzing. Second, MPFUZZ is iteratively run against the reduced mempool to discover short exploits. Third, MPFUZZ automatically extends the short exploits to actual ones that are functional on real mempools and Ethereum clients. Internally, the design of MPFUZZ is based on seven transaction symbols we design out of Ethereum semantics: future, parent, overdraft, latent overdraft, and replacement transactions. Under these symbols, in each iteration of fuzzing, MPFUZZ explores one concrete transaction per symbol, sends the generated transaction sequence to the target mempool,

¹For instance, future transactions can be caused by out-of-order information propagation in Ethereum.

observes the mempool end state, and extracts the feedback of symbolized state coverage and state promisingness in reaching bug oracles to guide the next round of fuzzing. In particular, MPFUZZ employs a novel technique to evaluate state promisingness, that is, by *optimistically* estimating the costs of unconfirmed transactions whose validity is subject to change in the future. After finding a short exploit against the reduced mempool, MPFUZZ automatically extends the small exploit to a more extensive exploit that is effective within a larger mempool. Specifically, MPFUZZ extracts all the unique admission event patterns in the small exploit and aligns these patterns to construct the attack transaction sequence on the larger-size mempool.

Found attacks: We run MPFUZZ on six leading execution-layer Ethereum clients deployed on the mainnet’s public-transaction path (Geth [10], Nethermind [11], Erigon [12], Besu [13], Reth [14], and OpenEthereum [15]), three PBS builders (proposer-builder separation) on the mainnet’s private-transaction and bundle path (Flashbot v1.11.5 [16], EigenPhi [17] and bloXroute [18]), and three Ethereum-like clients (BSC v1.3.8 [19] deployed on Binance Smart Chain, go-opera v1.1.3 [20] on Fantom, and core-geth v1.12.19 [21] on Ethereum Classic). On Ethereum clients of historical versions, MPFUZZ can rediscover known DETER bugs. On the latest Ethereum clients where DETER bugs are fixed, MPFUZZ can find new ADAMS attacks, described next.

We summarize the newly discovered ADAMS exploits into several patterns: 1) Indirect eviction by valid-turned-invalid transactions. Unlike the direct-eviction pattern used in DETER, the indirect-eviction attack works more stealthily in two steps: The attacker first sends normal-looking transactions to evict victim transactions from the mempool and then sends another set of transactions to *turn* the admitted normal-looking transactions into invalid ones, bringing down the cost. 2) Locking mempool, which is to occupy the mempool to decline subsequent victim transactions. Mempool locking does not need to evict existing transactions from the mempool as the eviction-based DETER attacks do. 3) Adaptive attack strategies where the attack composes adversarial transactions in an adaptive way to the specific policies and implementations of the mempool under test. Example strategies include composing transactions of multiple patterns in one attack, re-sending evicted transactions to evict “reversible” mempools, locking mempool patched against turning, etc.

All newly found ADAMS bugs are reported to the developer communities, including Ethereum Foundation, BSC, Fantom, PBS builders, etc. with 15 bugs confirmed and 4 fixed in recent client releases [22]. Bug reporting is documented on the webpage [23], which also includes demos of MPFUZZ on the tested Ethereum clients. MPFUZZ will be open-sourced to facilitate vulnerability discovery in more and future clients.

Systematic evaluation: We conducted an ablation study to evaluate the performance of MPFUZZ, which incorporates three distinct techniques. We aim to identify the contribution and significance of each component to the overall MPFUZZ. We implement four baseline fuzzers to compare against MPFUZZ. The first baseline is a stateless fuzzer built within the GoFuzz framework [24]. For the remaining three baselines, each one

selectively disables a single technique from MPFUZZ: symbolized state, symbolized input, and promising feedback and energy. The experimental result shows that the stateless fuzzer is the least effective in discovering ADAMS exploits. Among the three distinct techniques, the symbolized input technique improves efficiency more compared to that of the promising feedback and symbolized state coverage, and the state promisingness in feedback is more beneficial for performance than symbolized state coverage.

We systematically evaluate the attack success rate and cost of all the exploits found by MPFUZZ on the Ethereum testnet and a local network. Specifically, we evaluate a newly discovered eviction attack on Goerli testnet. The result of the eviction attack shows the Gas used by normal transactions significantly drops to 3.19% after the launch of the attack, which indicates that only a few normal transactions are included in the blocks following the attack. The locking attack evaluated on Goerli testnet shows the normal transactions received from the victim node drop essentially to zero, which indicates the locking attack is highly successful. Additionally, we evaluate other exploits on a local network. The evaluation results of all attacks on the Ethereum clients, PBS and Ethereum-like clients show that the attack success rates are all higher than 84.63%, and the attack costs are all lower than 1.172 Ether per block.

Contributions: The paper makes contributions as follows:

- *New fuzzing problem:* This paper is the first to formulate the mempool-fuzzing problem to automatically find asymmetric DoS vulnerabilities as bug oracles. Fuzzing mempools poses new unique challenges that existing blockchain fuzzers don’t address and entails a larger search space including invalid transactions and varying prices.
- *New fuzzing method:* The paper presents the design and implementation of MPFUZZ, a symbolized-stateful mempool fuzzer. Given a mempool implementation, MPFUZZ defines the search space by the mempool states covered under symbolized transaction sequences and efficiently searches this space using the feedback of symbolized state coverage and the promisingness of an intermediate state in triggering bug oracles. With a Python prototype and runs on real Ethereum clients, MPFUZZ achieves a $> 100\times$ speedup in finding known DETER exploits compared to baselines.
- *New discovery of mempool vulnerabilities:* MPFUZZ discovers new asymmetric-DoS vulnerabilities in six major Ethereum clients in the mainnet. By evaluation under real transaction workloads, all found attacks achieve 84.6 – 99.6% success rates and low costs such as adversarial transaction fees 100 \times lower than the victim transaction fees.
- *New discovery of mempool vulnerabilities:* MPFUZZ discovers new asymmetric-DoS vulnerabilities in six major Ethereum clients, PBS and Ethereum-like clients. We found and reported 24 newly discovered ADAMS bugs. After our reporting, 15 bugs are confirmed and 3 bugs are fixed.
- *New found attack evaluation:* This paper presents the evaluation results of the attack success rate and cost of all the exploits found by MPFUZZ on the Ethereum testnet and a local network. By evaluation under real transaction workloads, all found attacks achieve 84.6 – 99.6% success rates and low

costs such as adversarial transaction fees $100\times$ lower than the victim transaction fees.

2. RELATED WORKS

Consensus fuzzers: Fluffy [7] is a code-coverage based differential fuzzer to find consensus bugs in Ethereum Virtual Machines (EVM). Specifically, given an EVM input, that is, a transaction sequence, Fluffy sends it to multiple nodes running different Ethereum clients (e.g., Geth and OpenEthereum) for execution. 1) The test oracle in Fluffy is whether the EVM end states across these nodes are different, implying consensus failure. 2) Fluffy mutates ordered transaction sequences at two levels: it reorders/adds/deletes transactions in the sequence, and for each new transaction to generate, it randomly selects values in Gas limits and Ether amounts. For the data field, it employs semantic-aware strategies to add/delete/mutate bytecode instructions of pre-fixed smart contract templates. 3) Fluffy uses code coverage as feedback to guide the mutation.

Loki [8] is a stateful fuzzer to find consensus bugs causing crashes in blockchain network stacks. Specifically, Loki runs as a fuzzer node interacting with a tested blockchain node through sending and receiving network messages. 1) The test oracle in Loki is whether the tested blockchain node crashes. 2) The fuzzer node uses a learned model of blockchain network protocol to generate the next message of complying format, in which the content is mutated by randomly choosing integers and bit-flipping strings. In other words, the mutation in Loki is unaware of application level semantics. For instance, if the message is about propagating an Ethereum transaction, the transaction’s nonce, Ether amount, and Gas price are all randomly chosen; the sender, receiver, and data are bit flipped. 3) Loki records messages sent and received from the test node. It uses them as the state. New states receive positive feedback.

Tyr [9] is a property-based stateful fuzzer that finds consensus bugs causing the violation of safety, liveness, integrity, and other properties in blockchain network stacks. Specifically, in Tyr, a fuzzer node is connected to and executes a consensus protocol with multiple neighbor blockchain nodes. 1) The test oracle Tyr uses is the violation of consensus properties, including safety (e.g., invalid transactions cannot be confirmed), liveness (e.g., all valid transactions will be confirmed), integrity, etc. The checking is realized by matching an observed end state with a “correct” state defined and run by the Tyr fuzzer. 2) Tyr mutates transactions on generic attributes like randomly selecting senders and varying the amount of cryptocurrencies transferred (specifically, with two values, the full sender balance, and balance plus one). When applied to Ethereum, Tyr does not mutate Ethereum-specific attributes, including nonce or Gas price. It generates one type of invalid transaction, that is, the double-spending one, which in account-based blockchains like Ethereum are replacement transactions of the same nonce. 3) Tyr uses state divergence as the feedback, that is, the difference of end states on neighbor nodes receiving consensus messages in the same iteration. In Tyr, the states on a node include both the messages the node sent and received, as well as blocks, confirmed transactions, and other state information.

These existing blockchain fuzzers [7]–[9] cannot detect mempool DoS bugs and are different from this work. Briefly, mempool DoS does not trigger system crashes and can not be detected by Loki. Mempool content difference across nodes does not mean insecurity, and the mempool DoS bugs can not be detected by Fluffy (which detects consensus state difference). While Tyr aims to detect liveness and safety violations, their model of invalid transactions is rudimentary. Specifically, they only model double-spending transactions and cannot detect DETER bugs [1] that rely on more advanced invalid transactions, like future transactions and latent overdrafts.

Blockchain DoS: Blockchain DoS security has been examined at different system layers, including P2P networks [25]–[28], mining-based consensus [29], [30], and application-level smart contracts [31]–[33] and DApp (decentralized application) services [34]. These DoSes are not related to mempools and are orthogonal to this work.

For mempool DoS, a basic attack is by sending spam transactions with high fees to evict victim transactions of normal fees [2]–[5], which incur high costs to attackers. DETER [1] is the first asymmetric DoS on Ethereum mempool where the adversary sends invalid transactions of high fees (e.g., future transactions or latent overdrafts) to evict victim transactions of normal fees. Concurrent to this work is MemPurge [6] posted online in June 2023; in it, the attacker reconnects her adversarial future transactions and makes them latent-overdraft transactions. The DETER bugs have been fixed on the latest Ethereum clients such as Geth *v1.11.4*, as we tested them in July 2023. Both DETER and MemPurge are manually discovered.

3. BACKGROUND

Ethereum mempools: In Ethereum, users send their transactions to the blockchain network, which are propagated to reach validator nodes. On every blockchain node, unconfirmed transactions are buffered in the mempool before they are included in the next block or evicted by another transaction. In Ethereum 2.0, transactions are propagated in two fashions: public transactions are broadcast among all nodes, and private transactions are forwarded to selected nodes, more specifically, selected builders and proposers (as in PBS or proposer-builder separation). The mempool is present on both paths, and it is inside Ethereum clients such as Geth [10] and Nethermind [11] (handling public transactions), and Flashbot [16] (private transactions). On these clients, a mempool also serves many other downstream modules, including MEV searchers or bots (in PBS), Gas stations, RPC queries, etc.

Mempools on different nodes are operated independently and don’t need to synchronize as the consensus layer does. For instance, future transactions are not propagated, and the set of future transactions in the mempool on one node is different from another node.

The core mempool design is transaction admission: Given an initial state, whether and how the mempool admits an arriving transaction. In practice, example policies include those favoring admitting transactions of higher prices (and thus evicting or declining the ones of lower prices), transactions arriving earlier, certain transaction types (e.g., parent over child

transactions), and valid transactions (over future transactions). See different types of Ethereum transactions in § 4-A.

Transactions and fees: In Ethereum, Gas measures the amount of computations caused by smart contract execution. When preparing for transaction tx , the sender needs to specify *Gas* and *GasPrice*; the former is the maximal amount of computations allowed for running smart contracts under tx , and the latter is the amount of Ether per Gas the sender is willing to pay. After tx is included in a block, the actual amount of computations consumed by contract execution is denoted by *GasUsed*. The fees of transaction tx are the product of *GasUsed* and *GasPrice*, that is, $tx.\text{fee} = \text{GasUsed} * \text{GasPrice}$.

After EIP-1559 [35], *GasPrice* is divided into two components: *BasePrice* and *PriorityPrice*, that is, $\text{GasPrice} = \text{BasePrice} + \text{PriorityPrice}$. Blockchain nodes follow the Ethereum protocol to derive *BasePrice* from Gas utilization in recent blocks. The fees associated with the *BasePrice* are burnt upon transaction inclusion. *PriorityPrice* is set by the transaction sender.

4. THREAT MODEL AND BUG ORACLE

In the threat model, an attacker controls one or few nodes to join an Ethereum network, discovers and neighbors critical nodes (e.g., top validators, backends of an RPC Service, MEV searcher) if necessary, and sends crafted adversarial transactions to their neighbors. The attacker in this work has the same networking capacity as in DETER [1].

The attacker's goal is to disable the mempools on the critical nodes or all nodes in an Ethereum network and cause damage such as deployed or dropped transactions in block inclusion, produced blocks of low or zero (Gas) utilization, and disabled other downstream services like MEV searchers. In practice, this damage is beneficial to competing block validators, MEV searchers, and RPC services. Besides, the attacker aims to cause this damage at asymmetrically low costs, as will be described.

A. Notations

Transactions: In Ethereum, we consider two types of accounts: a benign account of index i denoted by B_i , and an adversarial account of index i denoted by A_i . A (concrete) Ethereum transaction tx is denoted by $tx[n^s v_f]$, where the sender is s , the nonce is n , the Gas price is f , and the transferred value in Ether is v . This work does not consider the “data” field in Ethereum transactions or smart contracts because smart contracts do not affect the validity of the Ethereum transaction. The notations are summarized in Table I.

TABLE I: Notations

Symbol	Meaning	Symbol	Meaning
m	Mempool length	ops	Tx sequence
st	State of residential txs in mempool	dc	History of declined txs from mempool
A	Adversarial tx sender	B	Benign tx sender
$tx[n^s v_f]$	A transaction from sender s , of nonce n , transferring Ether value v , and with Gas Price f		

We use each of the following symbols to represent a disjoint group of transactions. Informally, \mathcal{N} is a transaction sent

from a benign account, \mathcal{F} a future transaction, \mathcal{P} a parent transaction, \mathcal{C} a child transaction, \mathcal{O} an overdraft transaction, \mathcal{L} a latent overdraft transaction, and \mathcal{R} a replacement transaction. These symbols are formally specified in § 5.

Particularly, we use the notion of latent overdraft from the existing work [1], which indicates a child transaction that by itself does not overdraft but does overdraft when taking into account its parent transactions. Suppose Alice has a balance of 5 Ether and sends tx_1 of nonce 1 spending 2 Ether and tx_2 of nonce 2 spending 4 Ether. tx_2 is a latent overdraft.

States and transitions: We recognize two mempool-related states in Ethereum, the collection of transactions stored in mempool st , and the collection of declined transactions dc .

Suppose a mempool of state $\langle st_i, dc_i \rangle$ receives an arriving transaction tx_i and transitions to state $\langle st_{i+1}, dc_{i+1} \rangle$.

An arriving transaction can be admitted with eviction, admitted without eviction, or declined by a mempool. The three operations are defined as follows. 1) An arriving transaction tx_i is admitted with evicting a transaction tx'_i from the mempool, if $st_{i+1} = st_i \setminus tx'_i \cup tx_i, dc_{i+1} = dc_i$. 2) tx_i is admitted without evicting any transaction in the mempool, if $st_{i+1} = st_i \cup tx_i, dc_{i+1} = dc_i$. 3) tx_i is declined and does not enter the mempool, if $st_{i+1} = st_i, dc_{i+1} = dc_i \cup tx_i$.

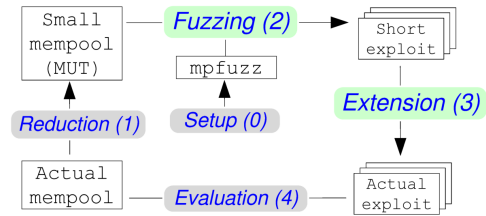


Fig. 1: Overview of exploit discovery and evaluation workflow: 0) MPFUZZ setup, 1) mempool reduction, 2) fuzzing on reduced mempool under test (MUT) to discover short exploits, and 3) exploit extension. The extended exploits are 4) evaluated on the actual mempool of the original size. Green means automated tasks, and gray requires manual effort.

B. Exploit Discovery Workflow

To set up the stage, we present the workflow overview in this work. The workflow is depicted in Figure 1. To discover vulnerabilities and exploits in an actual mempool, one has to 0) set up MPFUZZ by various parameters (as will be introduced), 1) reduce the mempool from its original configuration to a much smaller version, named mempool under test (MUT). 2) MPFUZZ is run on the reduced MUT deployed locally (with settings described in § 8-A). Fuzzing leads to the discovery of short exploits. 3) Short exploits are extended to the longer ones, that is, actual exploits. 4) The success of the actual exploit is evaluated on the actual mempools deployed in close-to-operational settings, such as using popular Ethereum testnets like Goerli (see § 7-A1) or a network we set up locally running unmodified Ethereum clients (see § 7-B2, § 7-C and § 7-D). Fuzzing a reduced mempool (MUT) instead of an original one is necessary to ensure the efficient execution of the MPFUZZ, which entails many iterations of re-initiating and populating the mempool.

In this workflow, fully automated is Step 2) and Step 3), that is, the discovery of short exploits on a given MUT and extension of the short exploit to an actual exploit (colored green in Figure 1). Other steps colored in gray require manual efforts and are described below: In **Step 0**, MPFUZZ setup entails setting parameters in bug oracles (e.g., ϵ and λ) and fixed symbols in guiding fuzzing. The setup is usually one-time. In **Step 1**), mempool reduction entails reconfiguring the mempool to a much smaller capacity (e.g., MUT length $m = 6$ or $m = 16$, compared to the original size like $m' = 6144$ as in Geth). In addition, policy-specific parameters in the actual mempool are tuned down proportionally. For instance, the Geth mempool buffers up to $py_1' = 1024$ future transactions, and when buffering more than $py_3' = 5120$ pending transactions, the mempool triggers a protective policy to limit the number of transactions sent from the same sender by $py_2' = 16$. In a reduced MUT of $m = 6$, these parameters are reduced while retaining the same proportion, such as $py_1 = 1, py_3 = 5, py_2 = 2$. The mempool reduction requires expert understanding and manual efforts, and it is by nature the best effort.

C. Bug Oracle: Definitions & Rationale

Definition 4.1 (Tx admission timeline): In a transaction admission timeline, a mempool under test is initialized at state $\langle st_0, dc_0 = \emptyset \rangle$, receives a sequence of arriving transactions ops , and ends up with state $\langle st_n, dc_n \rangle$. Then, a validator continually builds blocks by selecting and clearing transactions in the mempool until the mempool is empty. This transaction timeline is denoted by $\langle st_0, dc_0 = \emptyset \rangle, ops \Rightarrow \langle st_n, dc_n \rangle$.

The transaction admission timeline is simplified from the timeline that an operational mempool experiences where transaction arrival and block building can be interleaved.

We use two mempool-attack templates to define two bug oracles: an eviction-based DoS where adversarial transactions evict existing victim transactions in the mempool, and a locking-based DoS where existing adversarial transactions in the mempool decline arriving victim transactions.

Definition 4.2 (Eviction bug oracle): A transaction admission timeline, $\langle st_0, dc_0 = \emptyset \rangle, ops \Rightarrow \langle st_n, dc_n \rangle$, is a successful ADAMS eviction attack, if.f. 1) the admission timeline causes full damage, that is, initial state st_0 contains only benign transactions, ops are adversarial transactions, and the result end state st_n contains only adversarial transactions (in Equation 1), and 2) the attack cost is asymmetrically low, that is, the total adversarial transaction fees in the end state st_n to be charged are smaller, by a multiplicative factor ϵ , than the attack damage measured by the fees of evicted transactions in the initial state st_0 (in Equations 2 and 3). Formally,

$$st_0 \cap st_n = \emptyset \quad (1)$$

$$asym_E(st_0, ops) \stackrel{\text{def}}{=} \frac{\sum_{tx \in st_n} tx.\text{fee}}{\sum_{tx \in st_0} tx.\text{fee}} \quad (2)$$

$$asym_E(st_0, ops) < \epsilon \quad (3)$$

Definition 4.3 (Locking bug oracle): A transaction admission timeline, $\langle st_0 = \emptyset, dc_0 = \emptyset \rangle, ops \Rightarrow \langle st_n, dc_n \rangle$, is

a successful ADAMS locking attack, if.f. 1) the admission timeline causes full damage, that is, the mempool is first occupied by adversarial transactions (i.e., st_n contains only adversarial transactions) and then declines the arriving normal transactions (i.e., dc_n contains only normal transactions); the normal transactions and adversarial transactions are sent by different accounts (i.e., Equation 4), and 2) the attack cost is asymmetrically low, that is, the average adversarial transaction fees in the mempool are smaller, by a multiplicative factor λ , than the attack damage measured by the average fees of victim transactions declined (i.e., Equations 5 and 6). Formally,

$$\cup_{tx \in dc_n} tx.\text{sender} \cap \cup_{tx \in st_n} tx.\text{sender} = \emptyset \quad (4)$$

$$asym_D(ops) \stackrel{\text{def}}{=} \frac{\sum_{tx \in st_n} tx.\text{fee}/\|st_n\|}{\sum_{tx \in dc_n} tx.\text{fee}/\|dc_n\|} \quad (5)$$

$$asym_D(ops) < \lambda \quad (6)$$

Design rationale: Both definitions use the normal transaction fees to measure the attack damage because these fees are not collected by the validator in the timeline under attack and are collectible without attack. Specifically, the damage in Definition 4.2 is measured by the fees of normal transactions in st_0 which are evicted in end state st_n and which would not have been evicted had there been no adversarial transactions in ops . The damage in Definition 4.3 is measured by the fees of normal transactions in ops which are declined from end state st_n and which would not have been declined had there been no adversarial transactions in ops .

Both definitions are strict and require causing full damage, such as evicting or declining *all* normal transactions. Strict definitions are necessary to ensure that what is found as exploits on the small MUT is true positive and works on the actual mempool.

The targeted attacks by this work are denial of mempool service in feeding downstream validators with valid transactions sent from benign users. They are different from other forms of DoS in blockchains, including resource exhaustion via executing malicious smart contracts [6], [34].

Particularly, in the threat model of mempool DoS, we assume the validators are benign and functional in building blocks. Because in all Ethereum clients we know, transactions are admitted into mempool without execution (i.e., executing the smart contracts they invoke), *GasUsed* is not a factor in transaction admission.² Thus, our bug oracle does not vary *GasUsed*. Instead, all the transactions are fixed at 21000 Gas (i.e., as if they don't invoke smart contracts).³ This design significantly reduces the search space without loss in covering different mempool behaviors. Besides, our bug oracle does not model the effect of EIP1559 or *BasePrice*. Without modeling *BasePrice*, our bug oracle can still capture the alternative transaction fee (the product of *GasPrice* and 21000 Gas), which is still proportional to actual *tip* or damage on validator revenue.

²The further design rationale for admitting transactions without execution is that an Ethereum transaction *tx*'s *GasUsed* is non-deterministic unless the ordering of *tx* w.r.t. other transactions in the block is fixed and *tx* is executed.

³We may use price and fees interchangeably.

5. STATEFUL MEMPOOL FUZZING BY MPFUZZ

A. Transaction Symbolization

The key challenge in designing MPFUZZ is the large input space of transaction sequences. Recall that an Ethereum transaction consists of multiple attributes (sender, nonce, *GasPrice*, value, etc.), each defined in a large domain (e.g., 64-bit string). Exploring the raw transaction space is hard; the comprehensive search is inefficient, and randomly trying transactions as done in the state-of-the-art blockchain fuzzers (in § 2) is ineffective. **Intuition:** We propose symbolizing transactions for efficient and effective mempool stateful fuzzing. Our key idea is to map each group of concrete transactions, triggering an equivalent mempool behavior into a distinct symbol so that searching for one transaction is sufficient to cover all other transactions under the same symbol. Transaction symbolization is expected to reduce the search space from possible concrete transactions to the symbol space.

In this work, we manually design seven symbols to represent transactions based on the Ethereum “semantics”, that is, how different transactions are admitted by the mempool.

TABLE II: Symbols, transactions, and associated costs. Tx refers to the instantiated transaction under a given symbol.

Symbol	Description	Tx	<i>cost()</i>	<i>opcost()</i>
\mathcal{N}	Benign	$tx[B^* \frac{1}{3}]$	3	3
\mathcal{F}	Future	$tx[A^* \frac{1}{m+1 m+4}]$	0	0
\mathcal{P}	Parent	$tx[A^r \frac{1}{4, m+3}]$	$[4, m+3]$	$[4, m+3]$
\mathcal{C}	Child	$tx[\frac{A[1,r]}{\geq 2} \frac{1}{m+4}]$	$m+4$	1
\mathcal{O}	Overdraft	$tx[\frac{A[1,r]}{\geq 2} \frac{m+1}{m+4}]$	0	0
\mathcal{L}	Latent overdraft	$tx[\frac{A[1,r]}{\geq 2} \frac{m-1}{m+4}]$	0	0
\mathcal{R}	Replacement	$tx[\frac{A[1,r]}{1} \frac{m-1}{m+4}]$	$m+4$	0

Specification: Suppose the current state contains adversarial transactions sent from r accounts A_1, \dots, A_r . These accounts have an initial balance of m Ether, where m equals the mempool capacity (say $m = 1000$). The rationale is that these accounts can send at most m adversarial transactions, each minimally spending one Ether, to just occupy a mempool of m slots. A larger value of attacker balance is possible but increases the search space.

Symbol \mathcal{N} defines a transaction subspace covering any normal transactions sent from any benign account and of any nonce, namely $tx[B^* \frac{1}{*}]$. In MPFUZZ, Symbol \mathcal{N} is instantiated to concrete transactions of fixed *GasPrice* 3 wei and of value 1 Ether. That is, symbol \mathcal{N} is instantiated to transaction $tx[B^* \frac{1}{3}]$, as shown in Table II. Among all symbols, \mathcal{N} is the only symbol associated with benign sender accounts.

Symbol \mathcal{F} defines the transaction subspace of any future transaction sent from an adversarial account; the future transaction is defined w.r.t. the current state. MPFUZZ instantiates symbol \mathcal{F} to concrete transactions of nonce $m+1$, value 1 Ether, *GasPrice* $m+4$ wei, and any adversarial account A^* . The instantiating pattern for symbol \mathcal{F} is $tx[A^* \frac{1}{m+1 m+4}]$.

Symbol \mathcal{P} defines the transaction subspace of any parent transaction from an adversarial account w.r.t. the current

state. MPFUZZ instantiates \mathcal{P} to a transaction of Pattern $tx[A^r \frac{1}{4, m+3}]$. Here, the transaction is fixed with a *GasPrice* in the range $[4, m+3]$ wei, value at 1 Ether, and nonce at 1. The *GasPrice* of a future transaction (\mathcal{F}) is $m+4$ wei, which is higher than the price of a parent transaction (\mathcal{P}) in $[4, m+3]$ wei. The purpose is to ensure that a future transaction can evict any parent transaction during fuzzing.

Symbol \mathcal{C} defines the transaction subspace of any adversarial child transaction w.r.t. the state. MPFUZZ instantiates \mathcal{C} to a transaction of Pattern $tx[\frac{A[1,r]}{\geq 2} \frac{1}{m+4}]$. The instantiated child transaction is fixed at *GasPrice* of $m+4$.

Symbol \mathcal{O} defines the transaction subspace of any adversarial overdraft transaction w.r.t. state st . MPFUZZ instantiates \mathcal{O} to a transaction of Pattern $tx[\frac{A[1,r]}{\geq 2} \frac{m+1}{m+4}]$. Recall that all adversarial accounts have an initial balance of m Ether.

Symbol \mathcal{L} defines the transaction subspace of any adversarial latent-overdraft transaction w.r.t. state st . MPFUZZ instantiates \mathcal{L} to a transaction of Pattern $tx[\frac{A[1,r]}{\geq 2} \frac{m-1}{m+4}]$. All adversarial accounts have an initial balance of m Ether.

Symbol \mathcal{R} defines the transaction subspace of any adversarial “replacement” transaction w.r.t., the state. Unlike the symbols above, the transactions under Symbol \mathcal{R} must share the same sender and nonce with an existing transaction in the current state st . MPFUZZ instantiates \mathcal{R} to a transaction of Pattern $tx[\frac{A[1,r]}{1} \frac{m-1}{m+4}]$. Here, we simplify the problem and only consider replacing the transaction with nonce 1.

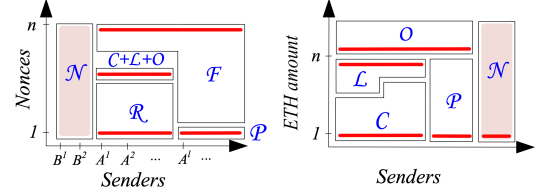


Fig. 2: Symbols and transaction space reduction.

Given that a concrete transaction in this work consists of four attributes, transactions are defined in a four-dimensional space. We visualize transaction symbols (with an incomplete view) in two two-dimensional spaces in Figure 2, that is, one of transaction sender and nonce and the other of sender and value. For each symbol, the figures depict the transaction subspace covered by the symbol (in white shapes of black lines) and the transaction pattern instantiated by MPFUZZ under the symbol (in red lines or shapes). In our design, the instantiated transactions are a much *smaller subset* of the defining transaction space. For instance, given state st of transactions sent from account A_1, \dots, A_r , transaction $tx[A_{r+1}^* \frac{1}{*}]$ is within the defining space of symbol \mathcal{F} , but MPFUZZ does not instantiate \mathcal{F} by transaction $tx[A_{r+1}^* \frac{1}{*}]$ (but instead to transactions $tx[A_{m+1}^* \frac{1}{m+4}]$).

1) *State Search Algorithm:* **Algorithm overview:** We propose a stateful fuzzing algorithm, listed in Algorithm 1, to selectively explore the input space in a way that prioritizes new and promising mempool states towards triggering ADAMS oracle.

The core data structure is a seed corpus or *sdb* which stores a list of input-state pairs or seeds. Upon running the algorithm, the corpus maintains the mempool states covered so far by the algorithm execution. The algorithm runs an outer loop

Algorithm 1 MPFUZZ(SeedCorpus sdb , Mempool mp)

```

1:  $sdb.init(mp);$ 
2: while  $\neg sdb.is\_empty()$  or timeout do
3:    $st, ops = sdb.next();$                                  $\triangleright$  Selection by energy
4:   for all  $ops', st' = mutateExec(ops, st)$  do
5:     if  $is\_ADAMS(st')$  then                           $\triangleright$  Test oracle
6:       emit( $ops', st'$ , "Found an exploit");
7:     else
8:       if  $\neg sdb.feedback(st', sdb)$  then
9:          $sdb.add(st', ops');$ 
10:      end if
11:    end if
12:   end for
13: end while

```

that continues until the corpus is empty, or only the states of zero energy are left, or timeout. In each iteration, the algorithm retrieves the next seed from the corpus based on how promising the seed is in reaching a state triggering the oracle (a.k.a., the energy [36]). A seed consists of a symbolized input ops , which consists of transaction symbols, and a symbolized state st reached by running a transaction sequence instantiated from the input ops (Line 3). The algorithm runs an inner loop, in each iteration of which it mutates the input in the current seed ((st, in)) and executes the mutated input against a reinitialized empty mempool, producing end state st' (Line 4). If the end state satisfies ADAMS conditions, it emits the mutated input-state pair ops', st' as a newly found exploit. The algorithm further checks the feedback: The feedback is positive if the mutated input ops' brings the mempool state st' closer to triggering the test oracle than st . This entails mutated state st' to be different from state st (i.e., increased state coverage) and state st' to achieve larger damage or lower attack cost. In case of positive feedback, the algorithm would add mutated input-state pair ops', st' to the corpus.

This algorithm assumes the mempool is deterministic. That is, given a seed $\langle ops, st \rangle$, running the same input ops against an empty mempool multiple times always results in the same end state st . In practice, we generate inputs to avoid the non-deterministic behavior of real mempool implementations.

The algorithm can be configured with initial seeds and input-mutation strategies. By default, we use one initial seed whose input fills up the mempool with normal transactions. The default input-mutation strategy is to append the current input with a newly generated transaction.

Algorithm 2 mutateExec(SymbolInput ops , SymbolState st)

```

1:  $ops' = mutateSymbol(ops);$ 
2:  $st_c = executeUnappended(ops, ops');$ 
3:  $st'_c = executeAppended(ops', st_c, st);$ 
4: return  $st'_c$ 

```

Input mutation: Given a symbolized input ops and symbolized state st , the mutation algorithm is to explore each “slightly” different input ops' and its associated state st' , such that the next stage can find the inputs producing positive feedback.

Internally, the algorithm proceeds at two levels, that is, symbols and concrete value. Specifically, as shown in Algorithm 2, 1) it appends the symbolized input ops with a previously untried symbol, generating the “mutated” symbolized input

ops' (Line 1 in Algorithm 2). In this step, the algorithm tries different symbols in the following order: $\mathcal{P}, \mathcal{L}, \mathcal{C}$. 2) It instantiates symbolized ops' to a transaction sequence and executes the sequence in the tested mempool to obtain the concrete end state (Line 2 in Algorithm 2). This step is necessary for instantiating and executing the mutation in the next step. Specifically, in this step, the algorithm instantiates symbolized input ops to a concrete input in_c , which is a sequence of transactions. It then drives the transactions to a reinitialized mempool for execution. It returns the resulting concrete state st_c . 3) The algorithm instantiates the appended symbols under the context of the previous state st and st_c . At last, it executes the appended transaction on mempool st_c to obtain the concrete end state st'_c under the mutated input (Line 3 in Algorithm 2).

Mutation feedback: We describe how mempool states are symbolized before presenting state-based feedback. In MPFUZZ, a symbolized state st is a list of transaction symbols, ordered first partially as follows: $\mathcal{N} \preceq \mathcal{E} \preceq \mathcal{F} \preceq \{\mathcal{P}, \mathcal{L}, \mathcal{C}\}$. \mathcal{E} refers to an empty slot. State slots of the same symbols are independently instantiated into transactions, except for $\mathcal{P}, \mathcal{C}, \mathcal{L}$. Child transactions (i.e., \mathcal{C}, \mathcal{L}) are appended to their parent transaction of the same sender (i.e., \mathcal{P}). Across different senders, symbols are ordered by the parent’s *GasPrice*. For instance, suppose a mempool stores four concrete transactions, $tx[\frac{A_1}{1} \frac{*}{4}]$, $tx[\frac{B}{100} \frac{*}{100}]$, $tx[\frac{A_2}{1} \frac{*}{5}]$, $tx[\frac{A_1}{2} \frac{*}{10001}]$, they are mapped to four symbols, $\mathcal{P}, \mathcal{F}, \mathcal{P}, \mathcal{C}$, and are further ordered in a symbolized state by \mathcal{FPCP} .

In MPFUZZ, the feedback of an input ops' is based on the symbolized end state st' . Positive feedback on state st' is determined conjunctively by two metrics: 1) State coverage that indicates state st' is not covered in the corpus, and 2) state promising-ness that indicates how promising the current state is to reach a state satisfying bug oracles.

$$feedback(st', st, sdb) = st_coverage(st', sdb) == 1 \wedge st_promising(st', st) == 1 \quad (7)$$

Specifically, state coverage is determined by straightforwardly comparing symbolized state st' , as an ordered list of symbols, with all the symbolized states in the corpus. For instance, state \mathcal{FPCP} is different from \mathcal{FPPC} . This also implies concrete transaction sequence $tx[\frac{A_1}{1} \frac{*}{4}], tx[\frac{B}{100} \frac{*}{100}], tx[\frac{A_2}{1} \frac{*}{5}], tx[\frac{A_1}{2} \frac{*}{10001}]$ is the same with $tx[\frac{A_1}{1} \frac{*}{4}], tx[\frac{B}{100} \frac{*}{100}], tx[\frac{A_2}{1} \frac{*}{6}], tx[\frac{A_1}{2} \frac{*}{10}]$, as they are both mapped to the same symbolized state.

How promising a state st' is (i.e., $st_promising(st')$) is determined as follows: A mutated state st' is more promising than an unmutated state st if any one of the three conditions is met: 1) State st' stores fewer normal transactions (under symbol \mathcal{N}) than state st , implying more transactions evicted and higher damage (i.e., $evict_normal(st', st) = 1$). 2) State st' declines (speculatively) more incoming normal transactions than state st , also implying higher damage (i.e., $decline_normal(st', st) = 1$). 3) The total fees of adversarial transactions in state st' are lower than those in state st , implying lower attack costs. We consider two forms of costs:

concrete cost and symbolized cost. The former, denoted by $cost(st')$, is simply the total fees of adversarial transactions instantiated from a symbolized state st' . The latter, denoted by $opcost(st')$, optimistically estimates the cost of transactions in the current state st' that contributes to a future state triggering test oracle. We will describe the symbolized cost next. Formally, state promising-ness is calculated by Equation 8.

$$\begin{aligned} st_promising(st', st) = & \ evict_normal(st', st) == 1 \vee \\ & \ decline_normal(st', st) == 1 \vee \\ & \ cost(st') < cost(st) \vee \\ & \ opcost(st') < opcost(st) \end{aligned} \quad (8)$$

Seed energy: Recall that in MPFUZZ, the next seed is selected from the corpus based on energy. By intuition, the energy of a state is determined based on how promising the state is in triggering the test oracle. In addition to the state promising-ness used in deciding feedback, state energy incorporates fuzz runtime information, such as how many times the state has been selected.

Specifically, the energy of a seed $\langle ops, st \rangle$ is determined by Equation 9.

$$Energy(in, st) = b / opcost(st) \quad (9)$$

First, each seed in the corpus records how many times it has been mutated. The more symbols it has mutated in the past, the less energy the seed currently has and the lower priority it will be selected next. b can be configured differently to traverse the state tree differently. In particular, breadth-first search (BFS) is by the following configuration: $b = 1$ if at least one symbol has not been tried (for mutation) in the current seed. Otherwise, $b = 0$.

Second, we use the symbolized cost to estimate how promising a state is and use it in seed energy.

Estimate state cost: When MPFUZZ determines how promising a state is, it needs to look beyond the current state and into all possible descendant states. We propose a heuristic that optimistically estimates the descendant-state costs given a current state. The key intuition is the following: In Ethereum, the validity of a child transaction (under symbol C) depends on its parent/ancestor transaction. Thus, even though a transaction in the current state is valid, the transaction can be “turned” into an invalid one in subsequent states. We thus attribute, optimistically, the cost of transaction C to value 1, so that it is preferable to a parent transaction P in input mutation and seed selection, and turning C into an invalid one like L or F is also encouraged. The cost profiles used in MPFUZZ are summarized in Table II.

B. Exploit Extension

The initial short exploit identified on MUT necessitates further automatic development to create a more extensive exploit that is effective within a larger mempool. The key idea in extending the small exploit to a more comprehensive one is to ensure the same admission event observed in the

smaller MUT. We first define the admission event as given an arriving transaction tx_i at a mempool of initial state st_0 , the admission of tx_i transitions the mempool into an end state tx_n . The admission event is denoted by $f(st_0, tx_i) \Rightarrow st_n$. We extract the admission event patterns, representing a state transition from the initial state to the end state. In the pattern, we only symbolize the mempool slots that are updated during the state transition. A pattern is denoted as $\langle st'_0, tx_i, st'_n \rangle$. For example, in the state transition from $NNPC$ to $NPPC$ by admitting a transaction P_0 , the symbolized state of a mempool slots transitions from N to P . Thus, we extract the pattern as $\langle N, P, P \rangle$.

we extract all the unique admission event patterns in the small exploit and store them into an admission event pattern set (aps). We then construct the attack transaction sequence on the larger-size mempool by aligning the patterns identified from the small exploit with corresponding admission events. This entails validating that the admission event pattern of a given event $f(st_0, tx_i) \Rightarrow st_n$ on the larger-size mempool exists within the aps . Specifically, MPFUZZ first selects api from the set aps whose initial state st_0 matches the state of the large mempool. We then instantiate tx_i of the api and send it to the large mempool. If the state transition of the large mempool $\langle st'_0, tx_i, st'_n \rangle$ aligns with the pattern api , this positive outcome prompts MPFUZZ to proceed with the extension process accordingly. Otherwise, MPFUZZ backtracks by rolling back the mempool state to its state prior to the admission of tx_i and tries the next pattern. MPFUZZ tries the patterns in the decreasing order of $opcost()$, which means if multiple admission event patterns in aps yield positive results, MPFUZZ proceeds the extension process by applying the pattern with the lower $opcost()$.

6. FOUND EXPLOITS

We have run MPFUZZ across a variety of Ethereum clients, including six leading execution-layer clients on the public-transaction path of Ethereum mainnet (Geth, Besu, Nethermind, Erigon, Reth, and OpenEthereum), three PBS clients (proposer-builder separation) on the mainnet’s private-transaction and bundle path (Flashbot builder v1.11.5 [16], EigenPhi builder [17] and bloXroute builder-ws [18]), and the clients deployed on three operational Ethereum-like networks (BSC v1.3.8 [19] deployed on Binance Smart Chain, go-opera v1.1.3 [20] on Fantom, and core-geth v1.12.19 [21] on Ethereum Classic).

On the six public-transaction clients, MPFUZZ leads to the discovery of 22 bugs, as listed in Table III, including 7 conforming to the known DETER attacks on clients of historical versions and 15 new bugs on the clients of the latest versions.

Other clients, including the three PBS clients and three clients on Ethereum-like networks, are mostly forks of the Geth clients, and on them, MPFUZZ discovered 13 bugs of a similar nature to those found on Geth (of the historical and latest versions), as seen in Table III.

We describe the patterns of these bugs as follows.

TABLE III: ADAMS exploit patterns found by MPFUZZ across Ethereum clients; XT_{1-7} are eviction based, and XT_{8-9} are locking based. XT_{1-3} are known patterns in DETER [1], while others are new. \times indicates the presence of a bug, \checkmark indicates the fixing of a bug after our reporting, and \checkmark indicates the fixing of a bug by previous works.

	XT_1	XT_2	XT_3	XT_4	XT_5	XT_6	XT_7	XT_8	XT_9
Geth $\geq v1.11.4$, Flashbot $\leq v1.11.5$, bloXroute, BSC $\leq v1.3.8$, core-geth $\leq v1.12.18$	\checkmark	\checkmark		\checkmark	\times	\times			
Geth $< v1.11.4$, EigenPhi go-opera $\leq v1.1.3$	\times	\times	\times	\times	\times	\times			
Erigon $\leq v2.42.0$					\times				
Besu $\geq v22.7.4$		\checkmark	\times		\times				
Besu $< v22.7.4$		\times	\times		\times				
Nethermind $\geq v1.18.0$		\checkmark			\times			\checkmark	
Nethermind $< v1.18.0$		\times			\times		\times		
Reth $\geq v0.1.0 - \text{alpha}.6$					\times			\checkmark	
Reth $< v0.1.0 - \text{alpha}.6$							\times		
OpenEthereum $\leq v3.3.5$					\times				\times

A. Found Eviction Attacks

Exploit XT_1 : Direct eviction by future transactions: In this attack, given a mempool’s initial state storing normal transactions, the attacker sends future transactions at high fees to evict the normal transactions. This exploit is essentially the DETER-X attack [1].

In practice, Geth ($\leq v1.11.4$), Nethermind, Besu, and EigenPhi are vulnerable under this exploit, as in Table III.

Exploit XT_2 : Direct eviction by latent overdraft transactions: In this eviction attack, the attacker sends latent-overdraft transactions at high fees to evict the normal transactions initially stored in the target mempool. These transactions are sent from k accounts, each of which sends l transactions, denoted by $k \times l$. The intention is to evade the limit on the number of transactions per sender. The evasion increases the attacker cost from one pending transaction to multiple. This exploit is essentially the DETER-Z attack [1].

In practice, Geth ($\leq v1.11.4$), Besu, EigenPhi, and go-opera are found vulnerable under this exploit.

Exploit XT_3 : Compositional direct eviction (by combining XT_1 and XT_2): In some Ethereum clients, notably Geth, the limit on the number of transactions per sender is triggered under the condition that the mempool stores enough pending transactions (e.g., more than 5120 transactions in Geth). This eviction attack combines XT_1 and XT_2 to avoid triggering the condition and evade the protection. It works by maximizing the eviction of mempool under XT_1 until it is about to trigger the condition. It then conducts XT_2 by sending latent overdraft transactions under one sender, that is, $1 \times l$. Compared to XT_2 , the combined exploit XT_3 achieves lower costs.

In practice, Geth ($\leq v1.11.4$) is vulnerable under this exploit where its mempool of capacity of 6144 slots triggers the limit of 16 transactions per sender when there are more than 5120 pending transactions. That is, XT_3 is configured with $l = 5120$. Other clients including EigenPhi and go-opera are also vulnerable.

Exploit XT_4 : Indirect eviction by valid-turned-overdraft transactions: This eviction attack works in two steps: 1) The attacker first sends valid transactions at high fees to evict normal transactions initially stored in the mempool. These transactions are sent from k accounts, each of which sends l transactions. 2) She then sends k transactions; each of the transactions is of nonce 1, at a high fee, of high value v_1 , and from the same k accounts in Step 1). The transactions

would replace the transaction of the same sender and nonce sent in Step 1). Once the replacement is finished, they turn their child transactions into latent overdraft. Specifically, if a sender’s balance is bal and the Ether value of transaction of nonce 2 is v_2 , then v_1 is carefully crafted to enable turned latent overdraft, that is, $v_1 < bal$ and $v_1 + v_2 > bal$.

In practice, many clients are found vulnerable under this exploit, including Geth $< v1.11.4$, Erigon, Besu, Nethermind, OpenEthereum, EigenPhi, and go-opera.

Exploit XT_5 : Indirect eviction by valid-turned-future transactions: This eviction attack works in two steps: 1) The attacker first sends valid transactions at high fees to evict normal transactions initially stored in the mempool. These transactions are sent by $k \times l$, that is, from k accounts, each with l transactions. For each sender, the transaction of nonce 1 has a fee, say f_1 , slightly lower than the transactions of other nonces, that is, $f_1 < f_2$. 2) She then sends k transactions; each of the transactions is from a distinct sender from those used in Step 1) and of fee f' that $f_1 < f' < f_2$. The intent is that the k transactions in Step 2) evict the transactions of nonce 1 sent in Step 1), turning other child transactions sent in Step 1) into future transactions.

Exploit XT_6 : Compositional indirect eviction (by multi-round valid-turned-future transactions): This exploit is an adaptive attack to the Geth $\geq v1.11.4$. Geth $\geq v1.11.4$ is patched against XT_{1-2} and adopts the following admission policies: The mempool of $m' = 6144$ slots admits up to $py'_1 = 1024$ future transactions. When containing more than $py'_3 = 5120$ pending transactions, the mempool starts to limit that no more than $py'_2 = 16$ pending transactions from the same sender can be admitted.

Exploit XT_6 works in three steps: 1) it first evicts the initial mempool of normal transactions with $m'/py'_2 = 384$ sequences, each of 16 transactions sent from one unique sender, 2) it then sends $py'_1/py'_2 = 64$ transactions to evict the parent transactions and creates $py'_1 = 1024$ future transactions in the mempool, 3) it sends one sequence of 5120 transactions from one sender to evict the normal transactions sent in Step 1), and 4) it sends one transaction to evict the parent transaction in Step 3), leaving the mempool of just one valid transaction. Step 3) can succeed because the precondition (w.r.t. $py'_3 = 5120$) of limiting transactions of the same sender does not hold.

In practice, Geth of all versions and the Geth forks, in-

cluding Flashbot, bloXroute, BSC, and Ethereum Classic are found vulnerable under XT_6 .

Exploit XT_7 : Reversible evictions: Suppose a mempool of state st admits an arriving transaction tx by evicting an existing transaction tx' , transitioning its state to st' . A mempool is reversible if one sends tx' to state st' , and the mempool admits tx' by evicting tx , transitioning its state back to st .

The mempool on Nethermind $< v1.18.0$ can be reversible: Minimally, suppose a two-slot mempool stores tx_1 of low fee from one sender and tx_2 of medium fee from another sender $A2$ and receives tx_3 as a child of tx_1 and of high fee. For instance, $tx_1[A \ 1]$, $tx_2[B \ 1]$, $tx_3[A \ 1]$. The Nethermind $< v1.18.0$ mempool would admit tx_3 and evict tx_2 . After that, if one resends the evicted tx_2 back to the mempool storing tx_1 and tx_3 , the Nethermind $< v1.18.0$ mempool would admit tx_2 and evict tx_3 , looping back to its initial state.

An attacker observing reversible mempool mounts Exploit XT_7 to evict the mempool while bringing down attack costs. On Nethermind $< v1.18.0$, the attack works in two steps: 1) She first sends k transaction sequences from k senders,⁴ each of l transactions (i.e., $k \times l$). In each l -transaction sequence, the nonce-1 transaction has a low fee, say f_1 , while all its child transactions are of high fees, evicting normal transactions initially stored in the mempool. 2) The attacker sends $k \times (l-1)$ transactions from $k \times (l-1)$ new senders, all with fees slightly higher than f_1 . The mempool would admit these transactions to the mempool by evicting all child transactions sent in Step 1), bringing down the attack costs.

B. Found Locking Attacks

Exploit XT_8 : Locking FIFQ: Certain mempool design prohibits eviction by admitting transactions as a FIFQ. Transactions are admitted to a mempool only when there are empty slots. A full mempool always declines an arriving transaction. In practice, Reth $v0.1.0 - alpha.4$ adopts the FIFQ mempool design.

While a FIFQ mempool can not be vulnerable to eviction attacks, it can be easily locked by Exploit XT_8 as follows: Whenever the attacker observes an empty slot present in the mempool, she sends a pending transaction of a minimally necessary fee to occupy the slot. Any transactions that arrive after will encounter a full mempool and are declined.

Exploit XT_9 : Locking mempool of no turning: Because of the risk of evicting a parent transaction that could lead to turning, certain mempool is designed to restrict eviction victims to child transactions; that is, only the transaction of maximal nonce under a given sender can be evicted. For instance, given an arriving transaction tx , the OpenEthereum mempool finds an existing child transaction tx' with a lower fee than tx and evicts it to admit tx .

In Exploit XT_9 , the attacker observes empty slots in the mempool (e.g., created by arriving blocks) and sends the same number of transactions to occupy them. The transactions are sent from one account where the child transaction has a

higher fee f_1 than normal transactions, while all its parent transactions have minimal fees. A normal transaction that arrives subsequently is declined because f_1 is higher than the fee of a normal transaction. Because each of its parent transactions has a low fee, the mempool is locked at a low cost.

7. ATTACK EVALUATION

A. Evaluation of Found Eviction Exploits on Testnet

We design experiments to measure the success of ADAMS attacks in real Ethereum networks.

1) Evaluation in Testnet: Experimental settings: We set up our experiment platform by connecting the attacker node to the Goerli testnet. The attacker node runs an instrumented Geth client at the execution layer which sends crafted transactions to the testnet.

To monitor transaction propagation, we launch an independent supernode (called measurement node) in the same testnet. The measurement node runs a reconfigured Geth client where the limit of peers/neighbors is removed and the measurement node can connect to as many neighbors as possible, hence a super node. The measurement node is not (directly) connected to the attacker node. When setting up our experiments, we ran the measurement node in Goerli for seven days and found the node is stabilized at 290 neighbors.

Block	Txn	Fee Recipient	Gas Used
0x00	178	0x56f155486299fecaff2d...	29,982,111 (99.94%)
0x00	22	0x00	8,854,501 (22.85%)
0x00	406	0x56f155486299fecaff2d...	Attack end 24,561,418 (81.87%)
0x00	389	0x56f155486299fecaff2d...	8,844,002 (21.89%)
0x00	466	0x045b5716359a857bc8...	8,844,002 (21.89%)
0x00	385	0xfffb65ebcd7e4307d2a...	8,844,002 (21.89%)
0x00	389	0xb64a303997fb0c154...	8,844,002 (21.89%)
0x00	37	0xc0e24599911fe27cc0...	Attack begin 8,503,438 (28.34%)
0x00	73	0xf0cf60b220cea3851a...	13,998,731 (46.66%)
0x00	33	0x000095e79eac4d76aa...	7,479,908 (24.93%)

Fig. 3: Mounting XT_4 attacks on Goerli: Etherscan screenshot of the blocks generated during the attack

Experiment results: The instrumented measurement node is able to log the received messages from different neighbors; these messages include those of transactions and of transaction hashes. The measurement node could receive the same transaction from different neighbors, and the log stores the transaction-neighbor pairs. We started logging the received messages one month before the experiment.

To do an experiment, we make the attacker node send XT_4 transactions using 384 accounts. Each account sends 16 valid pending transactions, followed by a replacement transaction. In total, the attacker node sends 6144 valid transactions and 384 replacement transactions. The *GasPrice* of the valid and replacement transactions are set to be 8 Gwei and 130 Gwei, respectively. Finally, we wrap up the experiment by waiting after the attacker node sends all messages and all replacement transactions are included in the blockchain.

Figure 3 shows the generated blocks in the experiment. We took the screenshot from etherscan.io and labeled it in red with information regarding the attack. Before the attack begins, the

⁴Nethermind does not limit transactions per sender, thus $k = 1$ in actual attacks.

testnet normally utilizes 24 – 47% of the Gas in a block. For ethics, our attacks are short (lasting four blocks).

Right after the launch of the attack, in block $xx07$, the Gas used by normal transactions drops to 3.19% and the Gas used by adversarial transactions (denoted by red bars in Figure 3) is 26.88%. The included adversarial transactions are 384 replacement transactions sent in the second round of XT_4 . The $6144 - 384 = 5760$ child transactions sent in the first round are not included in the block. Other blocks during the attack, namely $xx08$ and $xx10$, are similar. In the third block $xx09$, 73.1% Gas is spent on including 82 normal transactions. To explain it, we inspect the raw history of transactions arriving at and logged by our measurement supernode and found that out of the 82 included normal transactions, only 4 are present in the log, implying the other 78 normal transactions are private ones that were not broadcast to the measurement node. Notice that our attacks require no discovery of critical nodes as needed in [1].

B. Evaluation of Found Locking Exploits on Reth

Given Exploit XT_8 found on Reth, we manually extended it to two actual exploits on unmodified Reth’s mempool, XT_{8a} , and XT_{8b} .

1) Exploit Extension: Mempool in Reth v0.1.0 – alpha.4: Recall that the mempool is a FIFO queue: Any transaction residential in the mempool is never evicted, no matter how high an arriving transaction’s fee is. Besides, when there is an empty slot in its mempool, it requires that the transaction admitted must have fees higher than the latest block’s base fee.

Actual exploit XT_{8a} : In XT_8 , the attack cost increases with the block base fee. We manually propose a method to decrease the block base fee in Ethereum by mounting an eviction attack on the previous block. Specifically, in Ethereum (after EIP1559), given a recently produced block i , the base block fee of block $i + 1$ is calculated dynamically as follows:

$$BasePrice(i + 1) = BasePrice(i) * \left[\frac{7}{8} + \frac{1}{4} * \frac{GasUsed(i)}{BlockLimit} \right] \quad (10)$$

Therefore, if an eviction attack can persistently lower the Gas utilization of recent blocks, the current block fees can be reduced, which decreases the costs of locking attacks on the current block. In Exploit XT_{8a} , we mount a series of eviction attacks first and then a locking attack against the Reth node.

Specifically, suppose in a network of a Reth node and a block validator node, the XT_{8a} attacker first keeps sending eviction attacks directly to the validator node for several consecutive blocks. When observing the block base fees drop sufficiently, the attacker mounts the regular locking attack XT_8 against the Reth node.

2) Attack Evaluation on Reth: Experimental settings: We set up an experiment platform for evaluating locking attacks, on which an attacker node is connected to a victim non-validator node, which is also connected to a workload generator node and a victim validator node. The attacker node also maintains a direct connection to the victim validator. The

network topology is depicted in Figure 4. The non-validator node runs the Geth v1.11.4 client.

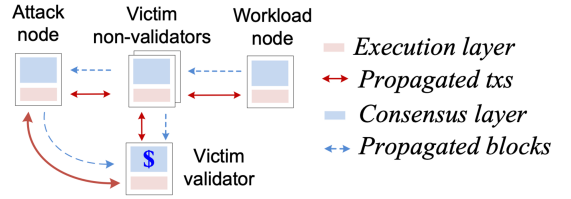


Fig. 4: Experimental setup for locking attacks on Reth

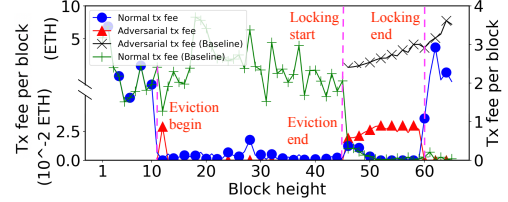


Fig. 5: Evaluation of locking attack XT_{8a} on Reth

Evaluation of XT_{8a} : To evaluate XT_{8a} , we set up the workload generator that sends normal transactions to the validator Geth node. The non-validator Reth node has not yet joined the network. We let the attacker node first send eviction attacks (XT_6) directly to the victim validator for 35 consecutive blocks until it observes the block base fees drop sufficiently to 1 Gwei, which occurs at the 45-th in our experiment. The Reth node then joins the network with an empty mempool. The attacker node mounts a locking attack XT_8 with transactions of price 5 Gwei to occupy the Reth node’s mempool.

We report the total fees of normal transactions included in the blocks – the lower the fees are, the more successful the locking attack is. We also report the adversarial transaction fees as the attack cost shown in Figure 5. When the locking attack begins at the 45-th block, the normal transaction fees increase because of the empty mempool on the Reth node which accepts some normal transactions in addition to the adversarial locking transactions. Then, after three blocks, the normal transaction fees quickly drop to near-zero Ether, showing the success of locking attacks. Interestingly, unlike the eviction attacks that cause low Gas utilization per block, the locking attacks just reduce the total Ether fees without reducing Gas utilization (i.e., the blocks produced under locking attacks from height 45 to 60 use the Gas of almost 100% block limit as shown in Figure 6). Due to the high Gas utilization, block base fees keep increasing during the locking attack. When reaching the 60-th block, the base fee is higher than the maximal transaction price tolerable by the attacker. In our experiment, the locking attacker stops at 60-th block, and the normal transaction fees immediately recover to the “normal” level. In practice, the attacker can repeat sending eviction attacks to reduce the base fee before mounting the locking attack again.

Figure 6 shows the Gas usage of attack transactions and normal transactions in XT_{8a} . During the locking attack from block height 45-th to 60-th, the attacker sends locking transactions to occupy all the empty slots. It makes the Gas usage of the attacker almost 100% block limit while the Gas usage of

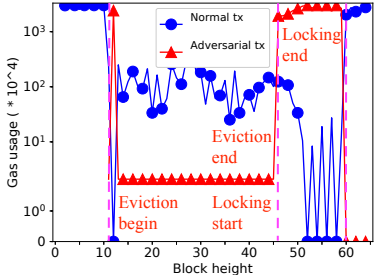


Fig. 6: Gas usage of attacks XT_{8a}

the normal transactions drops to around 0. When empty slots are created by arriving blocks, normal transactions compete with the attack transactions to admit into the empty slots. Thus, some normal transactions are included in blocks during the locking attack.

We also manually designed another locking variant for Reth. Suppose the Reth node does not run block validation, and its mempool is initially synchronized with the mempool of a block validator. The attacker first evicts 10,000 normal transactions from the validator's mempool. Then, the Reth node's mempool is permanently locked by the 10,000 normal transactions evicted from the validator mempool. Because these 10,000 transactions will never be included in blocks, they would exist in the Reth node's mempool forever, permanently locking it in its current state.

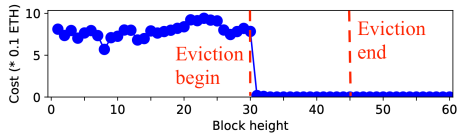


Fig. 7: Evaluation of locking attack XT_{8b} on Reth

Evaluation of XT_{8b} : To evaluate XT_{8b} , we initially set up the attacker node connected to the validator node running Geth, the workload generator node connected to the victim non-validator Reth node, and the Reth node connected to the validator. The system is run long enough to produce a certain number of blocks and the normal transactions are propagated to both validator and on-validator nodes' mempools. We then mount the eviction attack (XT_6) directly to the validator Geth node that evicts the mempool transactions on the validator node and prevents them from being included in the blocks.

By mounting eviction attacks between the 30-th to 45-th blocks in Figure 7, the Reth mempool is successfully locked afterward: From the figure, after the 45-th block, the total fees of normal transactions included in blocks remain at zero Ether per block until the experiment ends on the 60-th block.

C. Evaluation of Locking on Geth

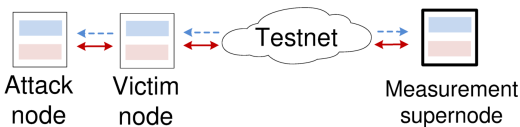


Fig. 8: Experimental setup for locking attacks on Geth/OpenEthereum

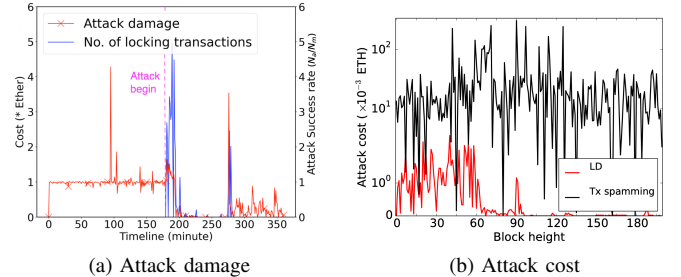


Fig. 9: Mounting locking attacks on a Geth node in testnet.

Design rational: Recall that OpenEthereum adopts an overly strict policy that determines eviction by only considering the fees of childless transactions. While this policy is intended to prevent turning attacks (XT_5), it is vulnerable to locking attacks. Because OpenEthereum has been deprecated from the operational Ethereum 2.0 networks, we re-implement its admission policy on Geth v1.11.4 and run the turning-hardened Geth on a victim under locking attacks.

Settings: We set up an experimental platform for evaluating locking attacks on Goerli testnet. The victim node runs the turning-hardened Geth client (based on v1.11.4) described above. The attacker node runs an instrumented Geth client (based on v1.11.4) at the execution layer such that it can mount locking attacks. Specifically, the Geth instrumentation enables the attacker node to monitor the local mempool and send a crafted transaction to the victim node upon each new empty slot created (by block arrival). The network topology is depicted in Figure 8.

In the experiment, we first run our three nodes for 350 minutes and then turn on the locking attack on the attacker node. We collect the benign transactions received by the attacker node (the number of which is denoted by N_a), the crafted transactions the attacker sends (the number denoted by N_c), and the benign transactions received by the measurement node (the number denoted by N_m). We use Metric $\frac{N_a}{N_m}$ to report the (inverse) of the attack success rate – Under the same transactions received by the measurement node, the fewer transactions the attacker node receives from the victim node, the more successful the victim mempool is locked.

Evaluation of locking attacks: We report in Figure 9a the locking attack's success rate over the period of 350 minutes. Each tick on the X axis represents 1 minute; that is, N_a/N_m is the number of benign transactions received by the attacker/measurement node every 1 minute. It is clear that the locking attack is highly successful – Right after the attack is launched at the 180-th minute, the rate of normalized transactions received from the victim node drops essentially to zero. And it persists over the period where the attack lasts.

We also calculate the attack cost by the total fees of the attacker's transactions included in the blockchain. In the experiment, we wait three hours after the attack stops and consider all the blocks produced until then. Not a single attacker's transaction sent in our experiment is included in the blockchain. This may be due to the low fee with which crafted transactions are sent.

Understanding crafted transaction inclusion is nondeterministic and dependent on benign transactions, we estimate the

worst-case attack cost, which is the total fees of crafted transactions sent by the attacker (i.e., when all the crafted transactions are included in the blockchain). Figure 9b reports the worst-case locking attack cost over time; on average, the attack, as successful as reported in Figure 9a, consumes 0.0004 Ether per block. By comparison, it is 0.028 Ether of transactions included per block, which is the minimal cost of the baseline transaction-spamming attack [2].

D. Evaluation of Found Exploits on Single Victim Node

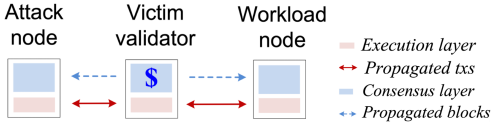


Fig. 10: Experimental setup

Evaluation settings: Our goal is to evaluate the success rate and cost of different ADAMS attacks on a single victim node. Because some ADAMS attacks are sensitive to the workload of normal transactions, we first collect transaction workloads from the mainnet. Specifically, we instrumented a Geth client (denoted by Geth-m) to log every message it receives from every neighbor. The logged messages contain transactions, transaction hashes (announcements), and blocks. When the client receives the same message from multiple neighbors, it logs it as multiple message-neighbor pairs. We also log the arrival time of a transaction or a block.

Workload collection: We launched a Geth-m node in the mainnet on May 17, 2023, turned on logging for 5 hours, and collected the transactions propagated to it. We make the collected transactions replayable as follows: We use the account balances and nonces on the mainnet to set up the initial state locally. We then replace the original sender in the collected transactions with the public keys that we generated. By this means, we know the secret keys of transaction senders and are able to send the otherwise same transactions for experiments.

For experiments, we set up three nodes, an attack node sending crafted transactions, a workload node sending normal transactions collected, and a victim node receiving transactions from the other two nodes. The victim node is connected to both the attack and workload nodes. There is no direct connection between the attack node and the workload node. The attacker node runs an instrumented Geth v1.11.4 client (denoted by Geth-a) that can propagate invalid transactions to its neighbors. The victim node runs the tested Ethereum client. The workload node runs a vanilla Geth v1.11.4 client. On each node, we also run a Prysm v3.3.0 client at the consensus layer. The experiment platform is denoted in Figure 10. Among the three nodes, we stake Ether to the consensus-layer client on the victim node, so that only the victim node would propose or produce blocks.

In each experiment, we first run the above “attacked” setup (i.e., with victim, attack and workload nodes). We then run a “regular” setup that excludes the attack node. Under the regular setup, the workload node sends the normal transactions and blocks to the victim node. We compare the experiment

results under the attacked setup and regular setup to show the success of the attack.

Evaluation of eviction/turning attacks on Single Node: We set up the experiment platform described in § 7-D. In each experiment, we drive benign transactions from the workload node. Note that the collected workload contains the timings of both benign transactions and produced blocks. On the 30-th block, we start the attack. Recall that each attack is configured by delay d ; the attack node observes the arrival of a produced block and waits for d seconds before sending a round of crafted transactions.

The attack phase lasts for 40 blocks; after the 70-th block, we stop the attack node from sending crafted transactions. We keep running workload and victim nodes for another 50 blocks and stop the entire process at the 120-th block. We collect the blocks produced and, given a block, we report two metrics: 1) total fees of benign transactions included, 2) total fees of attack transactions included.

In each experiment, we also re-run the workload and victim nodes with the same setup. In this “no-attack”, we don’t run the attack node. We collect the blocks produced, and, given a block, we report two metrics: 3) total fees of transactions included (denoted as “Benign ops - no attack”), and 4) the cost of a baseline spamming attack with 100% success rate (denoted as “Spamming - analytical”). For the latter, given a block, we select the transaction of the highest price, and report the price multiplied by the Ethereum block Gas limit.

Figure 11a reports the metrics for XT_6 on a victim node running Geth v1.11.4. Before the attack is launched (i.e., before the 30-th block), the two experiment runs (attacked and no attack) produce the blocks of the same benign transaction fees, i.e., around 2 – 3 Ether per block. As soon as the attack starts from the 30-th block, the benign transaction fees quickly drop to zero Ether except for some sporadic spikes (under 1 Ether per block). The non-zero Ether cost is due to that XT_6 cannot lock the mempool. The adversarial transaction fees show up and remain close to zero Ether per block. After the attack stops on 70-th block, the benign transactions under attack gradually recover to the level of transactions under no attack.

We also conduct experiments with varying attack delays between 0 and 12 seconds (note that the average time to produce a block in our collected trace is 14 seconds). Figure 11c shows the results of Attack XT_4 on Nethermind. On shorter delay than 8 seconds, the success rates are strictly 100%, and the attack cost remains at 0.025 Ether per block. When the delay grows over 8 seconds, success rates begin to drop, and attack costs increase. At the delay of 12 seconds, the success rate is 80%, and the attack cost is 1.5 Ether per block. The reason is that as the delay becomes large, the transaction sequence sent in an attack can be interrupted by block production, leading to adversarial transactions included in the blockchain and normal transactions un-evicted from the mempool.

The results of Attack XT_4 on Geth as shown in Figure 11e are similar to those on Nethermind. The difference is the cost of XT_4 on Geth is higher than that of Nethermind. In the attack sequence of XT_4 on Geth, it needs 384 attack senders which means 384 attack transactions are included in

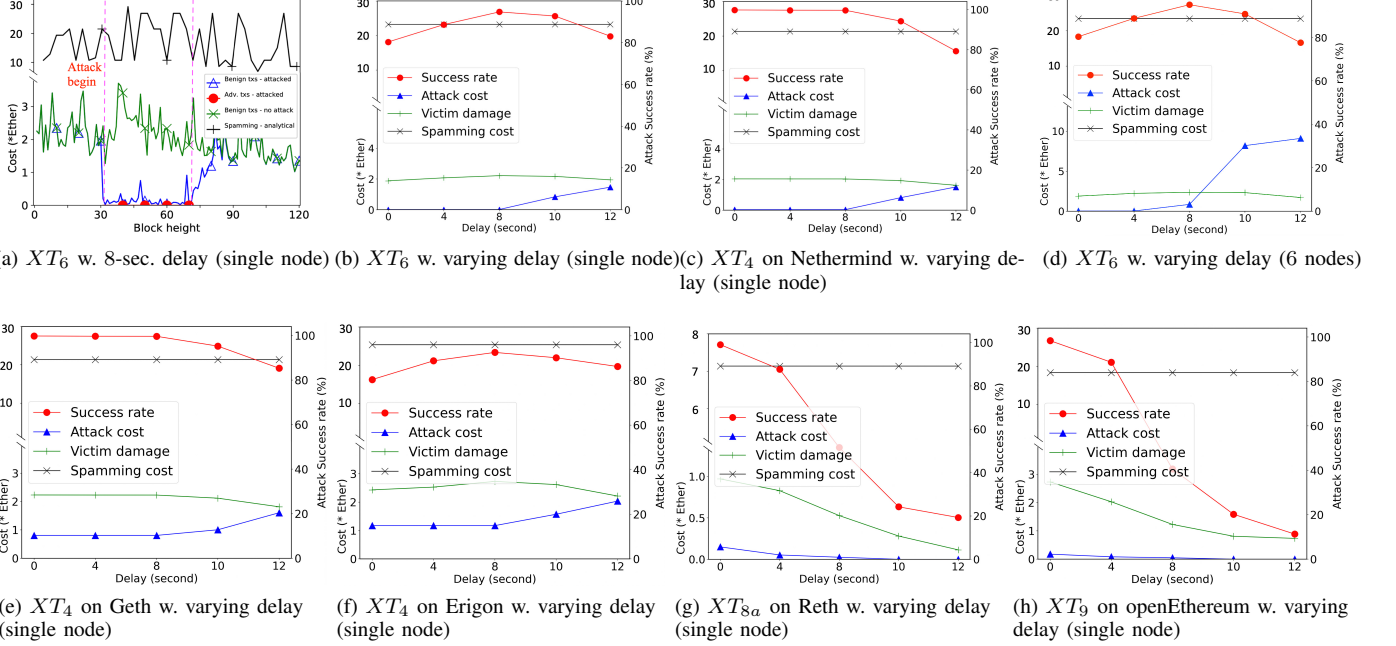


Fig. 11: Success rate and cost of turning-based eviction attack and locking attack.

blocks on shorter delay than 8 seconds while only 1 attack transaction is included in XT_4 on Nethermind. Figure 11b shows the success rates and costs of Exploit XT_6 on Geth v1.11.4. The results are similar to those in Figure 11c except that when the delay is short, the success rates of XT_6 are not 100% because XT_6 cannot lock the attacked mempool and an attack sent too early risks admitting normal transactions sent after the attack. The results of Attack XT_4 on Erigon are shown in Figure 11f. The results are similar to those in Figure 11b as the XT_4 on Erigon also cannot lock the attacked mempool when the delay is short. Figure 11g shows the success rates and cost of XT_8 on Reth. When the delay is 0 second, the success rate is 99.04%, and the cost is 0.151 Ether per block. The low-priced attack transactions sent with a 0 delay occupy all the empty slots and decline all the incoming normal transactions. When the delay grows, the success rate and attack cost begin to drop. The reason is as the delay increases, more empty slots in the mempool are occupied by normal transactions. As a result, more normal transactions and less attack transactions are included in blocks. The results of Attack XT_9 on OpenEthereum are shown in Figure 11h. The results are similar to those of XT_8 on Reth except when the delay is short, the cost of XT_9 on OpenEthereum is 0.177 per block which is higher than that of Reth. The reason is that each attack sender in the XT_9 attack sequence sends a high-priced child transaction for declining the incoming normal transactions and the high-priced transactions are included in blocks.

The evaluation results of all attacks on all clients are in Table IV. On the six Ethereum clients in the public transaction path, the attack success rates are all higher than 84.63%, and the attack costs are all lower than 1.172 Ether per block, which is significantly lower than the baseline.

On PBS clients and Ethereum-like clients, we also evaluate the attacks found by MPFUZZ. Under the same experimental settings as § 7-D, the results show similar success rates and costs with the attacks on Geth (recall these clients are Geth forks). More specifically, Table IV shows that the success rates are higher than 92.60%, and attack costs are lower than 0.806 Ether per block.

E. Evaluation of Found Exploits on Multi Nodes

Evaluation settings: We extend our experiment platform to support a network of victim nodes, instead of a single victim node. Specifically, the attack node is connected to the first victim non-validator node V_1 . Node V_1 is connected to the second victim non-validator node V_2 , which is further connected to node V_3 . The chain of victims continues until it reaches the 6-th non-validator victim V_6 , which is connected to the validator victim node V_0 . The workload node is connected to the validator node V_0 . We run the victim network among a set of geo-distributed cloud instances on the Internet. We place victim nodes V_1, V_3, V_5 in one geographic area in Amazon AWS cloud (a.k.a., one Availability Zone or AZ). We place the other victim nodes V_2, V_4, V_6, V_0 in a different geographic area, so that each message sent between V_i and V_{i+1} has to travel across continents on the Internet. The experiment architecture is illustrated in Figure 10.

Experiment results: On the multi-victim platform, we conduct similar experiments as in § 7-D. The results are presented in Figure 11d. Compared with the results on the single node, the attack cost increases faster and is much higher. For instance, when the delay is 10/12 seconds, the attack cost is 8/8.5 Ether per block, which is higher than the attack damage (i.e., the victim transaction fees). Under the delay, the attacks incur higher attack cost than damage and are no

TABLE IV: Attack success rate and cost

Clients	Exploit	Success rate	Cost (Ether/block)	Baseline (Ether/block)
Geth v1.10.25	XT_1	99.80%	0	11.39
	XT_2	99.42%	0.725	11.39
	XT_3	93.02%	0.0021	11.39
Geth v1.11.4	XT_4	99.42%	0.806	11.39
	XT_5	92.65%	0.806	11.39
	XT_6	94.74%	0.0022	11.39
Erigon v2.42.0	XT_4	92.53%	1.172	17.7
Nethermind v1.18.0	XT_4	99.60%	0.0021	10.75
Besu v22.7.4	XT_7	84.63%	0.20	10.75
	XT_2	99.63%	1.04	17.7
Reth v0.1.0-alpha.6	XT_4	99.60%	1.06	17.7
	XT_4	92.53%	0.672	17.6
Flashbot builder v1.11.5	XT_6	94.74%	0.0022	11.39
EigenPhi builder	XT_1	99.80%	0	11.39
	XT_2	99.42%	0.725	11.39
	XT_3	93.02%	0.0021	11.39
	XT_4	99.42%	0.806	11.39
	XT_6	94.74%	0.0022	11.39
bloXroute builder-ws	XT_6	94.74%	0.0022	11.39
go-oper v1.1.3	XT_2	99.12%	0.201	11.39
	XT_3	92.60%	0.0021	11.39
	XT_4	99.13%	0.221	11.39
	XT_6	93.76%	0.0022	11.39
BSC v1.3.8	XT_6	94.74%	0.0022	11.39
core-geth v1.12.18	XT_6	94.74%	0.0022	11.39
Reth v0.1.0-alpha.4	XT_8	99.04%	0.151	7.14
OpenEthereum v3.3.5	XT_4	99.56%	0.233	11.39
	XT_9	98.36%	0.177	18.35

longer ADAMS. By contrast, from Figure 11b, the attack costs on the single node with 10/12-second delays are 1/1.4 Ether per block, both of which are below the attack damage. The cause of the higher attack cost is the longer time to propagate the transaction sequence of an ADAMS attack in the multi-node setting than in the single node; the longer time implies the higher chance the transaction sequence is interrupted by the production of the next block and that the transactions are included to the block without being turned invalid.

8. EVALUATION OF MPFUZZ

A. Ablation Study

In this section, we describe 4 baseline fuzzers to demonstrate the performance efficacy of the techniques proposed in MPFUZZ as an ablation study.

Baseline B1 - stateless: We implement a stateless fuzzer in the GoFuzz framework. 1) Given a bit string generated by GoFuzz, the fuzzer code parses it into a sequence of transactions; the length of the sequence depends on the length of the bit string. It skips a bitstring that is too short. Specifically, when parsing the bitstring into transaction sequence, every 3 bits are parsed into one transaction, corresponding to 6 adversarial symbolized transactions proposed in MPFUZZ. 2) The fuzzer then sets up and initializes a Geth `txpool` instance with m normal transactions generated from the symbolized transaction \mathcal{N} . 3) The fuzzer sends the transaction sequence to the initialized mempool for execution. 4) It checks the

mempool state after execution: If the eviction-based test oracle (Equations 1, 2 and 3) is met, it emits the current transaction sequence as an exploit. 5) As a stateless fuzzer, it cannot use the same feedback technique as that of MPFUZZ. In contrast, it takes code coverage as feedback, specifically, if this run increases the code coverage in Geth client, the fuzzer adds the current bit-string to the seeds corpus.

Baseline B2a - non-symbolized state: Compared to MPFUZZ, the only difference is that the baseline B2a takes concrete state in the state coverage, while MPFUZZ takes symbolized state in the state coverage. Specifically, after sending the current transaction sequence to the mempool, it sorts the transactions in the mempool by senders and nonces. It then hashes the sorted transactions in the mempool and checks the presence of the hash digest in the seeds. If no hash exists, the current transaction sequence would increase the concrete-state coverage and be inserted into the corpus. However, the energy of a state is determined the same way as MPFUZZ. Specifically, given the concrete state that an input reaches, the energy is determined by its symbolized state.

Baseline B2b - non-symbolized input: We implement the third baseline fuzzer, which is also similar to MPFUZZ but without symbolized input mutation. In each iteration, the baseline fuzzer B2b appends to the current transaction sequence a new transaction. Given the m -slot mempool, the fuzzer tries m values for senders, m values for nonces, m values for Gas price, and m values for Ether amount. After sending to the mempool the current transaction sequence, it uses the same way to determine the feedback and energy as MPFUZZ.

Baseline B3 - non-promising feedback & energy We build the last baseline fuzzer, which is the same with MPFUZZ except that it removes the state promising-ness from its feedback and energy mechanism proposed in MPFUZZ from the seed selection. Specifically, the feedback formula in B3 includes only state coverage ($st_coverage$) and excludes state promisingness ($st_promising$ as in Equation 7). In addition, B3 uses as the energy the number of invalid transactions on a mempool state. The seed with more invalid transactions in the mempool has higher energy or priority to be selected for the next round of fuzzing.

Experimental settings of fuzzing: We run the four baselines and MPFUZZ against a MUT in a Geth client reconfigured under two settings: A small setting where the mempool is resized to 6 slots $m = 6$ and all fuzzers run for two hours (if test oracle is not triggered), and a medium setting where $m = 16$ and fuzzers run for 16 hours. The fuzzing experiments are run on a local machine with an Intel i7-7700k CPU of 4 cores and 64 GB RAM.

Results: Table V reports the time used that the first exploit is found under the small and medium MUT settings. For the small MUT of 6 slots, baseline B1 cannot find any attack in two hours, B2a, B2b and B3 can find the Exploit XT_3 in 0.10, 34.61 and 1.66 minutes respectively. By contrast, MPFUZZ finds the same exploit (XT_3) in 0.03 minutes.

For the medium setting, with 16 slots, baselines B1, B2b, and B3 cannot find any exploit in 16 hours, while B2a can find Exploit XT_3 in 0.26 minutes. By contrast, MPFUZZ finds the same exploit in 0.06 minutes.

The result that B1 has the poorest performance shows a stateless fuzzer would be ineffective in discovering ADAMS exploits. As B2a and B3 are more performant compared to B2b, it shows the symbolized input technique improves efficiency more compared to that of the promising feedback and symbolized state coverage. The comparison of results between B2a and B3 indicates that the state promisingness in feedback is more beneficial for performance than symbolized state coverage.

TABLE V: Fuzzing Geth v1.11.3’s mempool (in minutes) by different approaches to detect Exploit XT_3 . OT means overtime.

Settings	B1	B2a	B2b	B3	MPFUZZ
6slot-2h	OT	0.10	34.61	1.66	0.03
16slot-16h	OT	0.26	OT	OT	0.06

The other experiments, including true/false positive rates and additional performance evaluation evaluation on different clients can be found in Section 7.2 and Appendix C, available in the online supplemental material, and are identical to the original conference paper [37].

9. CASE STUDY: HOW MPFUZZ FINDS EXPLOITS IN MUT AND EXTENDS TO A LARGE MEMPOOL

We describe how MPFUZZ finds an exploit that evades the defense. We present a case study on finding XT_6 in the latest Geth $\geq v1.11.4$. Recall that a Geth mempool has a capacity of $m' = 6144$ slots, and its transaction-admission policies are characterized by three essential parameters: admitting up to $py'_1 = 1024$ future transactions and limiting up to $py'_2 = 16$ pending transactions from any senders when more than $py'_3 = 5120$ pending transactions are residing in the mempool. For ease of description, we set up the MUT to run the same codebase or the same admission policy but with different, smaller parameters: $m = 4, py_1 = 1, py_2 = 2, py_3 = 2$. We first describe how MPFUZZ finds a short exploit of XT_6 on the MUT. We then describe how MPFUZZ extends the short exploit into a longer version suitable for a medium-sized mempool.

Fuzzing: How MPFUZZ automatically finds exploits: Initially, the mempool is filled with $m = 4$ normal transactions. That is, the initial symbolized state is $NNNN$. The seed corpus sdb initially contains an empty string. To simplify the description, we only show Symbols C and P in the input mutation for ease of illustration. MPFUZZ retrieves the empty string and appends to it with different symbols C_0 and P_0 . Because of the initial state $NNNN$, only Symbol P_0 is feasible. It generates the mutated input P and instantiates it to a parent transaction of a higher fee than normal transactions (as described in § 5). Sending the input to the mempool gets the transaction admitted, leading to transitioned state $st_1 = NNNP$. This is a new state that is not in the corpus, and it evicts more normal transactions N than the previous state st_0 ; the input produces positive feedback, and the associated input-state pair $\langle P, st_1 = NNNP \rangle$ is added to the corpus.

Next, MPFUZZ retrieves from sdb a seed by high energy. According to Table II, the energy of state $NNNN$ is $\frac{1}{3*4}*0$, and the energy of state $NNNP$ is $\frac{1}{3*3+4}*1 = 1/13 > 0$. Hence,

seed $NNNP$ is selected. MPFUZZ tries input mutation and appends to the selected input P one of three new symbols, that is, C_1, P_0 or P_1 . On state $NNNP$, 1) Mutation transaction from C_1 is admitted, transitioning the state to $NNPC$, which produces positive feedback and is added to sdb . 2) Likewise, transaction P_0 is admitted and produces state $NNPP$ of positive feedback; the mutated input is also added to sdb . 3) Mutation P_1 is admitted but produces an identical state with mutation P_0 ; thus, the mutated input is not added to sdb .

Now, there are four seeds in sdb : $NNNN(0)$, $NNNP(0)$, $NNPC(1/11)$, and $NNPP(1/15)$. In parentheses are their energy numbers. The seed of the highest energy $NNPC(1/11)$ is selected (i.e., Step ① in Figure 12). MPFUZZ then mutates $NNPC$ with three possibilities, that is, C_1, P_0 , and P_1 , which produce two end states with positive-feedback, that is, $NPPC$ and $NPCC$. They are added to the sdb with energy $NPPC(1/13)$ and $NPCC(1/13)$.

Let’s say $NPPC(1/13)$ is selected (②). MPFUZZ then mutates input PC_1P_0 with five mutation transactions, that is, C_1, C_2, P_0, P_1, P_2 , which produces three end state with positive feedback, that is, $PCPC(1/11)$, $PPPC(1/16)$ and $PPCP(1/16)$. After that, $PCPC$ is chosen for the next-round fuzzing (③). Mutation P_2 is admitted and leads to state $FPCP$ with positive feedback. Similarly, upon state $FPCP$ (④), mutation C_2 is admitted and leads to state $FEPC$ (⑤). Then, C_1 transits the state to $FPCC$ (⑥). Upon state $FPCC$, mutation P_1 is admitted and leads to state $FEEP$ which satisfies the bug oracle of eviction attacks under $\epsilon = 0.34$. The algorithm then emits the found short exploit: $\langle st_0 = NNNN, dc_0 = \emptyset \rangle, ops = \mathcal{P}C_1P_0C_1P_2C_2C_1P_1$ (recall Definition 4.1). The snapshot of the state-search tree is depicted in Figure 12.

Exploit extension: Given the short exploit automatically found on MUT (with $m = 4, py_1 = 1, py_2 = 2, py_3 = 2$), the next step is to extend it to a longer exploit functional on larger mempool. We present a case study on extending the short exploit (XT_6 on MUT) to a longer exploit on a medium-size mempool (with $m = 8, py_1 = 2, py_2 = 3, py_3 = 6$). we extend the small exploit to the longer exploit by ensuring the same admission event occurs on the actual mempool as on the smaller MUT. To do so, we first extract all the unique admission event patterns $\langle st'_0, tx_i, st'_n \rangle$ in the small exploit and save them into an admission event pattern set (aep). Recall the admission event definition in § 5-B. In the XT_6 exploit found by MPFUZZ, we extract 6 patterns, including $\langle N, P, P \rangle$ from ①, $\langle N, C, C \rangle$ from ②, $\langle PC, P', P'F \rangle$ from ③, $\langle PC, C', C'E \rangle$

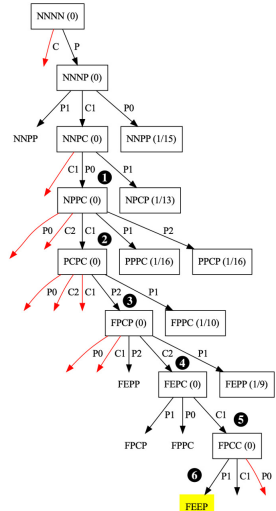


Fig. 12: Snapshot of the MPFUZZ state-search tree when finding Exploit XT_6 on Geth v1.11.4.

from ❸, $\langle \mathcal{EP}, \mathcal{C}, \mathcal{PC} \rangle$ from ❹, and $\langle \mathcal{PCC}, \mathcal{P}', \mathcal{P}'\mathcal{EE} \rangle$ from ❺.

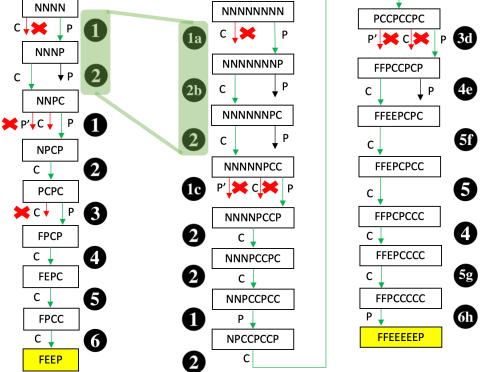


Fig. 13: Exploit XT_6 extension on Geth v1.11.4 with a medium-size mempool.

We then construct the attack transaction sequence on the larger-size mempool by aligning the patterns identified from the small exploit with corresponding admission events. Specifically, this entails verifying that the admission event pattern of a given event $f(st_0, tx_i) \Rightarrow st_n$ on the larger-size mempool is present within the aep . Initially, the mempool is filled with $m = 8$ normal transactions and the symbolized state is $NNNNNNNN$. There are two patterns in aep whose initial state st'_0 matches the mempool state, that is $\langle \mathcal{N}, \mathcal{P}, \mathcal{P} \rangle$ and $\langle \mathcal{N}, \mathcal{C}, \mathcal{C} \rangle$ (❶). Between these two patterns, only sending transaction \mathcal{P} is feasible. Therefore, MPFUZZ sends \mathcal{P} upon the initial state which leads to transitioned state $NNNNNNN\mathcal{P}$. In this admission event, the submission of transaction \mathcal{P} results in its admission in the mempool by evicting a \mathcal{N} in the initial state. Thus, it aligns the pattern of $\langle \mathcal{N}, \mathcal{P}, \mathcal{P} \rangle$. This positive outcome prompts MPFUZZ to proceed with the extension process accordingly.

Given the mempool state $NNNNNNNN\mathcal{P}$, there are two patterns in aep whose initial state st'_0 matches the mempool state, that is $\langle \mathcal{N}, \mathcal{P}, \mathcal{P} \rangle$ and $\langle \mathcal{N}, \mathcal{C}, \mathcal{C} \rangle$ (❷). Both of the tx_i in these two patterns are feasible. In this case, MPFUZZ applies the pattern that decreases the most $opcost()$ first. Recall the specification of the $opcost()$ in Table II. Thus, MPFUZZ applies the pattern $\langle \mathcal{N}, \mathcal{C}, \mathcal{C} \rangle$ that has the smaller $opcost()$ of the end state. Sending a \mathcal{C} leads to the admission of \mathcal{C} by evicting a \mathcal{N} , which aligns the end state of the pattern. Similarly, MPFUZZ extends another \mathcal{C} in the input transaction sequence and transitions the mempool state to $NNNNNNPCC$. At this time, there are 4 patterns whose initial state st'_0 matches the mempool state and is also feasible. In the $opcost()$ decreasing order, MPFUZZ first try to apply pattern $\langle \mathcal{PCC}, \mathcal{P}', \mathcal{P}'\mathcal{EE} \rangle$ by sending a \mathcal{P} . However, the mempool state led by admitting \mathcal{P} does not match the end state st'_n of the pattern. This negative outcome results MPFUZZ backtrack by rollback the mempool state before admitting \mathcal{P} , which is $NNNNNNPCC$. Similarly, the second pattern $\langle \mathcal{N}, \mathcal{C}, \mathcal{C} \rangle$ fails to transition the mempool state to correspond with the end state of the pattern. Consequently, MPFUZZ applies the next pattern $\langle \mathcal{N}, \mathcal{P}, \mathcal{P} \rangle$ transitions the mempool state to $NNNNNPCCP$ (❸).

Continuing the aforementioned process, MPFUZZ leads the mempool state to $PCCPCCPC$ (❹). Among the three patterns

whose initial state matches the mempool state, only applying $\langle \mathcal{P}, \mathcal{P}', \mathcal{P}'\mathcal{F} \rangle$ can get a corresponding end state in the state transition. That is, sending a \mathcal{P} results to the mempool state as $FFPCCP$. Subsequently, MPFUZZ selects the pattern $\langle \mathcal{P}, \mathcal{C}, \mathcal{C}' \rangle$, due to its lower $opcost()$ (❺) and then applies the only pattern that aligns the mempool state transition, which is $\langle \mathcal{EP}, \mathcal{C}, \mathcal{PC} \rangle$, resulting in the mempool state of $FF\mathcal{E}PCCP$ (❻). Similar to the aforementioned process, MPFUZZ leads the mempool state to $FFPCCCCC$ (❼). Upon that, MPFUZZ applies the only pattern that aligns the mempool state transition, which is $\langle \mathcal{PCC}, \mathcal{P}', \mathcal{P}'\mathcal{EE} \rangle$, and transitions the mempool state to $FFEEEEEP$ (❽). The mempool state satisfies the bug oracle of eviction attacks within the small mempool of MUT, satisfying the condition that $\epsilon \leq 0.34$. The algorithm then emits the extend exploit against the medium-size mempool, which is $ops = PCCPCCPCPCCC$.

10. DISCUSSIONS

Responsible bug disclosure: We have disclosed the discovered ADAMS vulnerabilities to the Ethereum Foundation, which oversees the bug bounty program across major Ethereum clients, including Geth, Besu, Nethermind, and Erigon. We also reported the found bugs to the developers of Reth, Flashbot, EigenPhi, bloXroute, BSC, Ethereum Classic and Fantom. Besides 7 DETER bugs that MPFUZZ rediscovered, 24 newly discovered ADAMS bugs are reported. As of March 2024, 15 bugs are confirmed: XT_1 (Nethermind, EigenPhi builder), XT_2 (EigenPhi builder), XT_3 (EigenPhi builder), XT_4 (Geth, Erigon, Nethermind, Besu, EigenPhi builder), XT_5 (Geth), XT_6 (Geth, Flashbot Builder, EigenPhi builder), XT_7 (Nethermind), and XT_8 (Reth). After our reporting, $XT_4/XT_7/XT_8$ have been fixed on Geth v1.11.4/Nethermind v1.21.0/Reth v0.1.0 – alpha.6. Bug reporting is documented [23].

Ethical concerns: When evaluating attacks, we only mounted attacks on the testnet and did so with minimal impacts on the tested network. For instance, our attack lasts a short period of time, say no more than 4 blocks produced. We did not test our attack on the Ethereum mainnet. Additionally, we obscure the first few digits of the block number in the attack screenshot, i.e., Figure 3. When reporting bugs, we disclose to the developers the mitigation design tradeoff and the risk of fixing one attacks by enabling other attacks (described above). To prevent introducing new bugs, we did not suggest fixes against turning-based locking (XT_5 , XT_6) and locking (XT_8).

11. CONCLUSION AND FUTURE WORKS

Conclusion: This paper presents MPFUZZ, the first mempool fuzzer to find asymmetric DoS bugs by exploring symbolized mempool states and optimistically estimating the promisingness of an intermediate state in reaching bug oracles. Running MPFUZZ on popular Ethereum clients discovers new mempool-DoS bugs, which exhibit various sophisticated patterns, including stealthy mempool eviction and mempool locking.

Limitations and future works: The exploit generation in this work is not fully automated. Manual tasks include mempool

reduction, MPFUZZ setup (configuring ϵ and symbols), etc. Automating these tasks is the future work.

MPFUZZ's bug oracles neither captures complete dependencies among concrete transactions nor guarantees completeness in finding vulnerabilities. Certified mempool security with completeness is also an open problem.

MPFUZZ targets a victim mempool of limited size: the vulnerabilities found in this work are related to transaction eviction, which does not occur in a mempool of infinite capacity. Thus, the MPFUZZ workflow cannot find exploits in the mempool of infinite capacity. It is an open problem whether a mempool of large or infinite capacity has DoS bugs.

12. ACKNOWLEDGMENTS

The authors thank the anonymous reviewers in USENIX security'24. The authors appreciate the discussion with Kangjie Lu in the early stage of this work. All authors but Kai Li are partially supported by two Ethereum Foundation academic grants and NSF grants CNS-2139801, CNS-1815814, DGE2104532. Kai Li is supported by NSF grant CNS2347486 and one Ethereum Academic Grant.

REFERENCES

- [1] K. Li, Y. Wang, and Y. Tang, "DETER: denial of ethereum txpool services," in *CCS '21: 2021 ACM SIGSAC Conference on Computer and Communications Security, Virtual Event, Republic of Korea, November 15 - 19, 2021*, Y. Kim, J. Kim, G. Vigna, and E. Shi, Eds. ACM, 2021, pp. 1645–1667. [Online]. Available: <https://doi.org/10.1145/3460120.3485369>
- [2] K. Baqer, D. Y. Huang, D. McCoy, and N. Weaver, "Stressing out: Bitcoin "stress testing"," in *Financial Cryptography and Data Security - FC 2016 International Workshops, BITCOIN, VOTING, and WAHC, Christ Church, Barbados, February 26, 2016, Revised Selected Papers*, ser. Lecture Notes in Computer Science, J. Clark, S. Meiklejohn, P. Y. A. Ryan, D. S. Wallach, M. Brenner, and K. Rohlloff, Eds., vol. 9604. Springer, 2016, pp. 3–18. [Online]. Available: <https://doi.org/10.1007/978-3-662-53357-4\1>
- [3] "Memoria 700 million stuck in 115,000 unconfirmed bitcoin transactions," <https://www.ccn.com/700-million-stuck-115000-unconfirmed-bitcoin-transactions/>, Retrieved July, 1, 2022.
- [4] M. Saad, L. Njilla, C. A. Kamhoua, J. Kim, D. Nyang, and A. Mohaisen, "Mempool optimization for defending against ddos attacks in pow-based blockchain systems," in *IEEE International Conference on Blockchain and Cryptocurrency, ICBC 2019, Seoul, Korea (South), May 14-17, 2019*. IEEE, 2019, pp. 285–292. [Online]. Available: <https://doi.org/10.1109/BLOC.2019.8751476>
- [5] "Report: Bitcoin (btc) mempool shows backlogged transactions, increased fees if so?" <https://goo.gl/LsU6Hq>, Retrieved May, 5, 2021.
- [6] A. Yaish, K. Qin, L. Zhou, A. Zohar, and A. Gervais, "Speculative denial-of-service attacks in ethereum," *Cryptology ePrint Archive*, Paper 2023/956, 2023, <https://eprint.iacr.org/2023/956>. [Online]. Available: <https://eprint.iacr.org/2023/956>
- [7] Y. Yang, T. Kim, and B. Chun, "Finding consensus bugs in ethereum via multi-transaction differential fuzzing," in *15th USENIX Symposium on Operating Systems Design and Implementation, OSDI 2021, July 14-16, 2021*, A. D. Brown and J. R. Lorch, Eds. USENIX Association, 2021, pp. 349–365. [Online]. Available: <https://www.usenix.org/conference/osdi21/presentation/yang>
- [8] F. Ma, Y. Chen, M. Ren, Y. Zhou, Y. Jiang, T. Chen, H. Li, and J. Sun, "LOKI: state-aware fuzzing framework for the implementation of blockchain consensus protocols," in *30th Annual Network and Distributed System Security Symposium, NDSS 2023, San Diego, California, USA, February 27 - March 3, 2023*. The Internet Society, 2023. [Online]. Available: <https://www.ndss-symposium.org/ndss-paper/loki-state-aware-fuzzing-framework-for-the-implementation-of-blockchain-consensus-protocols/>
- [9] Y. Chen, F. Ma, Y. Zhou, Y. Jiang, T. Chen, and J. Sun, "Tyr: Finding consensus failure bugs in blockchain system with behaviour divergent model," in *2023 2023 IEEE Symposium on Security and Privacy (SP) (SP)*. Los Alamitos, CA, USA: IEEE Computer Society, may 2023, pp. 2517–2532. [Online]. Available: <https://doi.ieee.org/10.1109/SP46215.2023.00068>
- [10] "Geth: the go client for ethereum," <https://www.ethereum.org/cli\#geth>.
- [11] "Nethermind ethereum client," <https://nethermind.io/client>.
- [12] "Erigon," <https://github.com/ledgerwatch/erigon>.
- [13] "Hyperledger besu," <https://www.hyperledger.org/use/besu>.
- [14] "Reth: Modular, contributor-friendly and blazing-fast implementation of theethereum protocol," <https://github.com/paradigmxyz/reth>.
- [15] "Parity ethereum is now openethereum: Fast and feature-rich multi-network ethereum client," <https://www.parity.io/ethereum/>.
- [16] "Flashbots mev-boost block builder," <https://github.com/flashbots/block-builder>.
- [17] "Eigenphi builder," <https://github.com/eigenphi/block-builder>.
- [18] "bloxroute builder," <https://github.com/bloxroute-Labs/block-builder-ws>.
- [19] "Bsc client," <https://github.com/bnb-chain/bsc>.
- [20] "go-operा," <https://github.com/Fantom-foundation/go-operा/tree/master>.
- [21] "core-geth," <https://github.com/etclabscore/core-geth>.
- [22] "Link hidden for anonymous paper submission."
- [23] "Flashbots block builder," <https://sites.google.com/view/mpfuzz>, Retrieved Oct, 2023.
- [24] "Go fuzzing," <https://go.dev/security/fuzz/>, Retrieved May 31, 2023.
- [25] E. Heilman, A. Kendler, A. Zohar, and S. Goldberg, "Eclipse attacks on bitcoin's peer-to-peer network," in *USENIX Security 2015*, Washington, D.C., USA, J. Jung and T. Holz, Eds. USENIX Association, 2015, pp. 129–144. [Online]. Available: <https://www.usenix.org/conference/usenixsecurity15>
- [26] Y. Marcus, E. Heilman, and S. Goldberg, "Low-resource eclipse attacks on ethereum's peer-to-peer network," *IACR Cryptology ePrint Archive*, vol. 2018, p. 236, 2018. [Online]. Available: <http://eprint.iacr.org/2018/236>
- [27] M. Apostolaki, A. Zohar, and L. Vanbever, "Hijacking bitcoin: Routing attacks on cryptocurrencies," in *IEEE Symposium on SP 2017*, 2017, pp. 375–392. [Online]. Available: <https://doi.org/10.1109/SP.2017.29>
- [28] M. Tran, I. Choi, G. J. Moon, A. V. Vu, and M. S. Kang, "A Stealthier Partitioning Attack against Bitcoin Peer-to-Peer Network," in *To appear in Proceedings of IEEE Symposium on Security and Privacy (IEEE S&P)*, 2020.
- [29] M. Mirkin, Y. Ji, J. Pang, A. Klages-Mundt, I. Eyal, and A. Juels, "Bdos: Blockchain denial of service," 2019.
- [30] "Irreversible transactions: Finney attack," https://en.bitcoin.it/wiki/Irreversible_Transactions\#Finney_attack, Retrieved July, 1, 2022.
- [31] D. Pérez and B. Livshits, "Broken metre: Attacking resource metering in EVM," in *27th Annual Network and Distributed System Security Symposium, NDSS 2020, San Diego, California, USA, February 23-26, 2020*. The Internet Society, 2020. [Online]. Available: <https://www.ndss-symposium.org/ndss-paper/broken-metre-attacking-resource-metering-in-evm/>
- [32] V. Buterin, "Eip150: Gas cost changes for io-heavy operations." [Online]. Available: <https://github.com/ethereum/EIPs/blob/master/EIPS/eip-150.md>
- [33] "Known attacks - ethereum smart contract best practices," https://consensys.github.io/smart-contract-best-practices/known_attacks\#dos-with-block-gas-limit, Retrieved May, 5, 2021.
- [34] K. Li, J. Chen, X. Liu, Y. R. Tang, X. Wang, and X. Luo, "As strong as its weakest link: How to break blockchain dapps at RPC service," in *28th Annual Network and Distributed System Security Symposium, NDSS 2021, virtually, February 21-25, 2021*. The Internet Society, 2021. [Online]. Available: <https://www.ndss-symposium.org/ndss-paper/as-strong-as-its-weakest-link-how-to-break-blockchain-dapps-at-rpc-service/>
- [35] "Transaction pricing mechanism eip1559," <https://github.com/ethereum/EIPs/blob/master/EIPS/eip-1559.md>, Retrieved Nov. 20, 2021.
- [36] J. Ba, M. Böhme, Z. Mirzamomen, and A. Roychoudhury, "Stateful greybox fuzzing," in *31st USENIX Security Symposium, USENIX Security 2022, Boston, MA, USA, August 10-12, 2022*, K. R. B. Butler and K. Thomas, Eds. USENIX Association, 2022, pp. 3255–3272. [Online]. Available: <https://www.usenix.org/conference/usenixsecurity22/presentation/ba>
- [37] Y. Wang, Y. Tang, K. Li, W. Ding, and Z. Yang, "Understanding ethereum mempool security under asymmetric dos by symbolized stateful fuzzing," 2024.